Spin diffusion in ultracold spin-orbit-coupled ^{40}K gas

T. Yu and M. W. Wu*

Hefei National Laboratory for Physical Sciences at Microscale, Key Laboratory of Strongly-Coupled Quantum Matter Physics and Department of Physics, University of Science and Technology of China, Hefei, Anhui 230026, China

(Received 19 April 2015; published 6 July 2015)

We investigate the steady-state spin diffusion for ultracold spin-orbit-coupled ^{40}K gas by the kinetic spin Bloch equation approach both analytically and numerically. Four configurations, i.e., the spin diffusions along two specific directions with the spin polarization perpendicular (transverse configuration) and parallel (longitudinal configuration) to the effective Zeeman field are studied. It is found that the behaviors of the steady-state spin diffusion for the four configurations are very different, which are determined by three characteristic lengths: the mean free path l_τ, the Zeeman oscillation length l_Ω, and the spin-orbit coupling oscillation length l_α. It is analytically revealed and numerically confirmed that by tuning the scattering strength, the system can be divided into *five* regimes: I, weak scattering regime ($l_\tau \gtrsim l_\Omega, l_\alpha$); II, Zeeman field-dominated moderate scattering regime ($l_\Omega \ll l_\tau \ll l_\alpha$); III, spin-orbit coupling-dominated moderate scattering regime ($l_\alpha \ll l_\tau \ll l_\Omega$); IV, relatively strong scattering regime ($l_\tau^c \ll l_\tau \ll l_\Omega, l_\alpha$); V, strong scattering regime ($l_\tau \ll l_\Omega, l_\alpha, l_\tau^c$), with l_τ^c representing the crossover length between the relatively strong and strong scattering regimes. In different regimes, the behaviors of the spacial evolution of the steady-state spin polarization are very rich, showing different dependencies on the scattering strength, Zeeman field and spin-orbit coupling strength. The rich behaviors of the spin diffusions in different regimes are hard to understand in the framework of the simple drift-diffusion model or the direct inhomogeneous broadening picture in the literature. However, almost all these rich behaviors can be well understood by means of our *modified* drift-diffusion model and/or *modified* inhomogeneous broadening picture. Specifically, several anomalous features of the spin diffusion are revealed, which are in contrast to those obtained from *both* the simple drift-diffusion model and the direct inhomogeneous broadening picture.

DOI: 10.1103/PhysRevA.92.013607 PACS number(s): 67.85.−d, 51.10.+y, 03.75.Ss, 05.30.Fk

I. INTRODUCTION

In recent years, spin dynamics including spin relaxation and spin diffusion and/or transport is extensively studied in both Bose [1–8] and Fermi [9–32] cold atoms. For the Bose system, the spin dynamics of the Bose-Einstein condensation has attracted much attention [1–8]. For the Fermi cold atoms, the systems without [9–25] and with [26–32] spin-orbit coupling (SOC) are extensively investigated. In the absence of the SOC, many interesting phenomena, such as the Leggett-Rice effect in unitary gas [17–21] and anomalous spin segregation in an extremely weak scattering limit [22–25], have enriched the understanding of the spin dynamics of Fermions. With the synthetic SOC experimentally realized by laser control technique in cold atoms [7,8,26,27], the spin relaxation for the Fermi cold atoms with SOC has been studied both experimentally [26–28] and theoretically [29–32]. This is partly motivated by the well-controlled laser technique, which provides more freedom for the cold atoms than the conventional solids. On one hand, rich regimes can be realized by tuning the SOC strength; on the other hand, not only can the interatom interaction be tuned by the Feshbach resonance [33], but also the atom-disorder interaction can be introduced and controlled by the speckle laser technique [34–38].

The experimentally realized effective Zeeman field and SOC provide an effective magnetic field, which reads [7,26,27]

$$\Omega(\mathbf{k}) = (\Omega, 0, \delta + \alpha k_x). \tag{1}$$

In above equation, $\mathbf{k} = (k_x, k_y, k_z)$ denotes the center-of-mass momentum of the atom; Ω acts as an effective Zeeman field along the $\hat{\mathbf{x}}$ direction; δ is the Raman detuning, which is set to zero in our work; and $\Omega_z(\mathbf{k}) = \alpha k_x$ represents the $\mathbf{k}$-dependent effective magnetic field along the $\hat{\mathbf{z}}$ direction, which is perpendicular to the Zeeman field, with $|\alpha|$ being the strength of the spin-orbit-coupled field. With this specific effective magnetic field $\Omega(\mathbf{k})$, by setting $\delta = 0$, it has been revealed that both the conventional [29,30,32] and anomalous [31,39,40] D'yakonov-Perel' (DP) [41] spin relaxations can be realized with $\langle|\Omega_z(\mathbf{k})|\rangle \gtrsim \Omega$ and $\langle|\Omega_z(\mathbf{k})|\rangle \ll \Omega$, respectively. For the conventional situation, in the strong (weak) scattering limit when $\langle|\Omega(\mathbf{k})|\rangle\tau_k^* \ll 1$ [$\langle|\Omega(\mathbf{k})|\rangle\tau_k^* \gtrsim 1$], the spin relaxation time (SRT) τ_s is inversely proportional (proportional) to the momentum scattering time τ_k^*. $\langle\cdots\rangle$ here denotes the ensemble average. For the anomalous situation [31,39,40] it has been found that by tuning the interatom interaction, the transverse spin relaxation can be divided into four regimes: the normal weak scattering ($\tau_s \propto \tau_k^*$), the anomalous DP-like ($\tau_s^{-1} \propto \tau_k^*$), the anomalous Elliott-Yafet (EY)-like [42,43] ($\tau_s \propto \tau_k^*$), and the normal strong scattering ($\tau_s^{-1} \propto \tau_k^*$) regimes. The longitudinal spin relaxation can be divided into two: i.e., the anomalous EY-like and the normal strong scattering regimes [39].

In contrast to the spin relaxation, the study for the spin diffusion in cold atoms with SOC has not yet been reported in the literature. However, the experimental configuration realized by Brantut *et al.* [44] for the "charge" diffusion of cold atoms can be applied to the spin diffusion straightforwardly. In their experiment, by adding the "barrier" laser in the middle of the cold atoms, the system is separated to the left and right parts. In the left part, the spin-polarized cold atoms

*Author to whom correspondence should be addressed: mwwu@ustc.edu.cn

can be prepared [26–28,32], whereas in the right part, the system remains in the equilibrium state. Specifically, the atom densities in the left and right parts are prepared to be the same. With the SOC introduced to the right part [26–28,32], i.e., the spin-diffusion region, by removing the "barrier" laser, this configuration can be used to study spin diffusion along one direction for the three-dimensional (3D) Fermi gas with SOC.

In the coordinate defined in Eq. (1), there are two specific configurations with the spin diffusions along the $\hat{\mathbf{x}}$ and $\hat{\mathbf{y}}$ directions, respectively. Accordingly, in the scattering-free situation, the $\mathbf{k}$-dependent spin precession frequencies in the spacial domain, i.e., the inhomogeneous broadening [45,46] in the steady-state spin diffusion along the $\hat{\mathbf{x}}$ and $\hat{\mathbf{y}}$ directions are determined by

$$\boldsymbol{\omega}^x(\mathbf{k}) = m\boldsymbol{\Omega}(\mathbf{k})/k_x = (m\Omega/k_x, 0, m\alpha), \tag{2}$$

$$\boldsymbol{\omega}^y(\mathbf{k}) = m\boldsymbol{\Omega}(\mathbf{k})/k_y = (m\Omega/k_y, 0, m\alpha k_x/k_y), \tag{3}$$

respectively [47,48]. Here m is the atom mass. From Eq. (2) [Eq. (3)], it can be seen that, in contrast to the spin relaxation in the time domain, in inhomogeneous broadening in the spacial domain, the original $\mathbf{k}$-independent Zeeman field Ω becomes $\mathbf{k}$-dependent, whereas the $\mathbf{k}$-dependent spin-orbit-coupled field $m\alpha k_x$ becomes $\mathbf{k}$ independent (remains $\mathbf{k}$ dependent). Hence, for the spin diffusion along the $\hat{\mathbf{x}}$ direction, the inhomogeneous broadening $\boldsymbol{\omega}^x(\mathbf{k})$ is similar to the one for spin relaxation in time domain $\boldsymbol{\Omega}(\mathbf{k})$ with one $\mathbf{k}$-independent magnetic field perpendicular to another $\mathbf{k}$-dependent one. Accordingly, rich regimes may exit in the steady-state spin diffusion along the $\hat{\mathbf{x}}$-direction for both the spin polarizations perpendicular and parallel to the Zeeman field. Whereas for the spin diffusion along the $\hat{\mathbf{y}}$ direction, from the different inhomogeneous broadenings in Eqs. (2) and (3), its behavior should be very different from the one along the $\hat{\mathbf{x}}$ direction.

In the present work, we investigate the steady-state spin diffusion for the 3D ultracold spin-orbit-coupled ^{40}K gas by the kinetic spin Bloch equation (KSBE) approach [45], both analytically and numerically. Four configurations, i.e., the spin diffusion along the $\hat{\mathbf{x}}$ and $\hat{\mathbf{y}}$ directions for the spin polarization $\mathbf{P}$ perpendicular ($\mathbf{P} \parallel \hat{\mathbf{z}}$, transverse configuration) and parallel ($\mathbf{P} \parallel \hat{\mathbf{x}}$, longitudinal configuration) to the Zeeman field are studied. It is shown analytically that the behaviors of the steady-state spin diffusion for the four configurations are very different, which are determined by three characteristic lengths: the mean free path $l_\tau = k\tau_k/m$, the Zeeman oscillation length $l_\Omega = k/(\sqrt{3}m\Omega)$, and the SOC oscillation length $l_\alpha = 1/(m|\alpha|)$. The spin-diffusion lengths for the spin diffusions in the four configurations are derived in the strong scattering regime, which are then extended to the weak scattering one. We further find that, by dividing the system into different regimes, the complex analytical results can be reduced to extremely simple forms. It is revealed that by tuning the scattering, the system can be divided into *five* regimes: I, weak scattering regime ($l_\tau \gtrsim l_\Omega, l_\alpha$); II, Zeeman field-dominated moderate scattering regime ($l_\Omega \ll l_\tau \ll l_\alpha$); III, SOC-dominated moderate scattering regime ($l_\alpha \ll l_\tau \ll l_\Omega$); IV, relatively strong scattering regime ($l_\tau^c \ll l_\tau \ll l_\Omega, l_\alpha$); V, strong scattering regime ($l_\tau \ll l_\Omega, l_\alpha, l_\tau^c$). Here l_τ^c represents the crossover length between the relatively strong and strong scattering regimes. In different regimes, the behaviors of the spacial evolution of the steady-state spin polarization are very rich, showing different dependencies on the scattering strength, Zeeman field and SOC strength. These dependencies are summarized in Tables I and II for the spin diffusions along the $\hat{\mathbf{x}}$ and $\hat{\mathbf{y}}$ directions, respectively.

The rich behaviors of the spin diffusions in different regimes are hard to understand in the framework of the previous simple drift-diffusion model [49–54] or the direct inhomogeneous broadening [Eqs. (2) and (3)] picture [45–48,55] in the literature. In the simple drift-diffusion model, there are only two rather than *five* regimes: the strong scattering regime with $l_s \propto 1/(m|\alpha|)$ and the weak scattering regime with $l_s \propto k\sqrt{\tau_k}/m$. In the present work, it is found that the behaviors of the spin diffusions can be analyzed in the situation either with strong Zeeman and weak spin-orbit-coupled fields (regimes II and V) or weak Zeeman and strong spin-orbit-coupled fields (regimes III and IV). Accordingly, our previous inhomogeneous broadenings [Eqs. (2) and (3)] should be extended to the *effective* ones. It is found that when the spin polarization is parallel to the larger field between the Zeeman and spin-orbit-coupled fields, the spin polarization cannot precess around the effective inhomogeneous broadening fields efficiently. In this situation, the previous drift-diffusion model is applicable but $\tau_s(\mathbf{k})$ modified as follows (*modified* drift-diffusion model). In the strong scattering regime, $\tau_s(\mathbf{k})$ remains the SRT in the conventional DP mechanism [29,30,32,45], whereas in the moderate scattering regime, $\tau_s(\mathbf{k})$ is replaced by the helix spin-

TABLE I. Behaviors of the steady-state spin polarization in the spatial domain and corresponding spin-diffusion lengths for configurations $\hat{\mathbf{x}}$-T and $\hat{\mathbf{x}}$-L in different regimes [$l_{\tau,x}^c \approx \sqrt{3}l_\alpha^2/(2l_\Omega)$].

Regime	Condition	Behavior and L_T^x in $\hat{\mathbf{x}}$-T	Behavior and L_L^x in $\hat{\mathbf{x}}$-L
I: Weak scattering regime	$l_\tau \gg l_\Omega, l_\alpha$	NA	NA
II: Zeeman field-dominated moderate scattering regime	$l_\Omega \ll l_\tau \ll l_\alpha$	Oscillation decay, $2l_\tau/\sqrt{3}$	Single exponential decay, $l_\tau l_\alpha/(\sqrt{3}l_\Omega)$
III: SOC-dominated moderate scattering regime	$l_\alpha \ll l_\tau \ll l_\Omega$	Single exponential decay, $l_\tau l_\Omega/(\sqrt{3}l_\alpha)$	Oscillation decay, $\sqrt{2}l_\tau l_\Omega/(\sqrt{3}l_\alpha)$
IV: Relatively strong scattering regime	$l_\tau \ll l_\alpha, l_\Omega$ and $l_\tau \gg l_{\tau,x}^c$ ($l_\tau \ll l_\alpha \ll l_\Omega$)	Single exponential decay, l_α	Oscillation decay, $\sqrt{2l_\tau l_\Omega/\sqrt{3}}$
V: Strong scattering regime	$l_\tau \ll l_\alpha, l_\Omega$ and $l_\tau \ll l_{\tau,x}^c$	Oscillation decay, $\sqrt{2l_\tau l_\Omega/\sqrt{3}}$	Single exponential decay, l_α

TABLE II. Behaviors of the steady-state spin polarization in the spacial domain and corresponding spin-diffusion lengths for configurations $\hat{\mathbf{y}}$-T and $\hat{\mathbf{y}}$-L in different regimes [$l^c_{\tau,y} \approx 4l_\alpha^2/(\sqrt{3}l_\Omega)$].

Regime	Condition	Behavior and L_T^y in $\hat{\mathbf{y}}$-T	Behavior and L_L^y in $\hat{\mathbf{y}}$-L
I: Weak scattering regime	$l_\tau \gg l_\Omega, l_\alpha$	NA	NA
II: Zeeman field-dominated moderate scattering regime	$l_\Omega \ll l_\tau \ll l_\alpha$	Oscillation decay, $\sqrt{2}l_\tau$	Single exponential decay, $l_\tau l_\alpha/(\sqrt{3}l_\Omega)$
III: SOC-dominated moderate scattering regime	$l_\alpha \ll l_\tau \ll l_\Omega$	Single exponential decay, $\sqrt{3}l_\tau l_\Omega/(2l_\alpha)$	Single exponential decay, l_α
IV: Relatively strong scattering regime	$l_\tau \ll l_\alpha, l_\Omega$ and $l_\tau \gg l^c_{\tau,y}$ ($l_\tau \ll l_\alpha \ll l_\Omega$)	Single exponential decay, $\sqrt{3}l_\tau l_\Omega/(2l_\alpha)$	Single exponential decay, l_α
V: Strong scattering regime	$l_\tau \ll l_\alpha, l_\Omega$ and $l_\tau \ll l^c_{\tau,y}$	Oscillation decay, $\sqrt{\sqrt{3}l_\tau l_\Omega}$	Single exponential decay, l_α

flip rates determined in the helix space [31,40]. When the spin polarization is perpendicular to the larger field between the Zeeman and spin-orbit coupled fields, the spin polarization can rotate around the effective inhomogeneous broadening fields efficiently. Hence, the behavior of the spin diffusion is determined by the *effective* inhomogeneous broadenings together with the spin-conserving scattering (*modified* inhomogeneous broadening picture). By means of the modified drift-diffusion model and modified inhomogeneous broadening picture, apart from regime IV, all the features in different regimes can be well obtained.

Several anomalous features of the spin diffusion, which are in contrast to those obtained from *both* the simple drift-diffusion model and the direct inhomogeneous broadening picture, are revealed. In the scattering strength dependence, it is found that when $l_\alpha \ll l_\Omega$, the longitudinal spin diffusion along the $\hat{\mathbf{y}}$ direction is *robust* against the scattering in a wide range including both the strong and the *weak* scattering regimes. In the Zeeman field dependence, when the system is in regime II, the *longitudinal* spin diffusion is enhanced by the Zeeman field. In the SOC strength dependence, we find that the spin-diffusion length can be also enhanced by the SOC in regime III. All these anomalous behaviors have been well understood from our modified drift-diffusion model and/or modified inhomogeneous broadening picture.

This paper is organized as follows. In Sec. II, we set up the model and KSBEs. In Sec. III, we show the analytical results for the transverse and longitudinal spin diffusion along the $\hat{\mathbf{x}}$ and $\hat{\mathbf{y}}$ directions. Different dependencies of the spin-diffusion length on the mean free path, Zeeman oscillation length and SOC oscillation length are revealed. In Sec. IV, both the analytical and the numerical calculations for the steady-state spin diffusion in 3D isotropic speckle disorder are presented. Specifically, the disorder strength (Sec. IV A), Zeeman field strength (Sec. IV B), and SOC strength (Sec. IV C) dependencies are discussed. We conclude and discuss in Sec. V.

II. MODEL AND KSBES

With the 3D disordered speckle potential introduced to the spin-diffusion region [34–38], the Hamiltonian of the spin-orbit coupled ultracold atom, which is composed by the effective Hamiltonian $\hat{H}_0$ [26,27], the disordered speckle potential $U(\mathbf{r})$ [34–38,44], and the interatom interaction $\hat{H}_{\rm int}$, is written as

$$\hat{H} = \hat{H}_0 + U(\mathbf{r}) + \hat{H}_{\rm int}. \tag{4}$$

The effective Hamiltonian consists of the kinetic energy of the atom and the SOC ($\hbar \equiv 1$),

$$H_0 = \mathbf{k}^2/(2m) + \mathbf{\Omega}(\mathbf{k}) \cdot \boldsymbol{\sigma}/2, \tag{5}$$

with $\boldsymbol{\sigma}$ being the vector composed of the Pauli matrices. The interaction Hamiltonian $\hat{H}_{\rm int}$ is approximated by the s-wave interatom scattering [30,56–59]. In our study, the scattering length is tuned to zero by the Feshbach resonance [33–38,44], and hence $\hat{H}_{\rm int}$ is absent in our following discussion.

The KSBEs, derived via the nonequilibrium Green function method with the generalized Kadanoff-Baym ansatz [45,46,60–62], are utilized to study the spin diffusion in the ultracold Fermi gas:

$$\partial_t \rho_{\mathbf{k}}(\mathbf{r},t) = \partial_t \rho_{\mathbf{k}}(\mathbf{r},t)|_{\rm dif} + \partial_t \rho_{\mathbf{k}}(\mathbf{r},t)|_{\rm coh} + \partial_t \rho_{\mathbf{k}}(\mathbf{r},t)|_{\rm scat}. \tag{6}$$

In these equations, $\rho_{\mathbf{k}}(\mathbf{r},t)$ represents the density matrices of atom with momentum $\mathbf{k}$ at position $\mathbf{r} = (x,y,z)$ and time t, in which the diagonal elements $\rho_{\mathbf{k},\sigma\sigma}$ describe the atom distribution functions and the off-diagonal elements $\rho_{\mathbf{k},\sigma-\sigma}$ represent the correlation between the spin-up and -down states.

For the quasi-1D spin diffusion, the diffusion term is written as

$$\partial_t \rho_{\mathbf{k}}(\mathbf{r},t)|_{\rm diff} = -(k_\zeta/m)\partial_\zeta \rho_{\mathbf{k}}(\mathbf{r},t), \tag{7}$$

with $\zeta = x$ or y for the spin diffusion along the $\hat{\mathbf{x}}$ or $\hat{\mathbf{y}}$ direction, respectively. The coherent term is given by

$$\partial_t \rho_{\mathbf{k}}(\mathbf{r},t)|_{\rm coh} = -i[\Omega(\mathbf{k}) \cdot \boldsymbol{\sigma}/2, \rho_{\mathbf{k}}(\mathbf{r},t)], \tag{8}$$

where [,] denotes the commutator.

The scattering terms $\partial_t \rho_{\mathbf{k}}(\mathbf{r},t)|_{\rm scat}$ represent the atom-disorder scattering [38]. In our study, the effective Zeeman splitting energy and the SOC energy are much smaller than the Fermi energy [63]. Moreover, in this work, we focus on the situation where the disorder strength is below the critical one satisfying the Ioffe-Regel condition [64], and hence the Anderson localization is not considered [65]. Hence, the atom-disorder scattering reads

$$\partial_t \rho_{\mathbf{k}}|^{\rm ad}_{\rm scat} = 2\pi \sum_{\mathbf{k}'} |U_{\mathbf{k}-\mathbf{k}'}|^2 \delta(\varepsilon_{\mathbf{k}} - \varepsilon_{\mathbf{k}'})(\rho_{\mathbf{k}'} - \rho_{\mathbf{k}}), \tag{9}$$

where

$$|U_{\mathbf{q}}|^2 = \iint d\mathbf{r}d\mathbf{r}'\langle[U(\mathbf{r})-U_0][U(\mathbf{r}')-U_0]\rangle e^{-i\mathbf{q}\cdot(\mathbf{r}-\mathbf{r}')} = \iint d\mathbf{r}d\mathbf{r}' C(\mathbf{r}-\mathbf{r}')e^{-i\mathbf{q}\cdot(\mathbf{r}-\mathbf{r}')} \equiv C_{\mathbf{q}}. \quad (10)$$

In Eq. (10), U_0 is the average value of the disorder potential. For the 3D isotropic disordered speckle [34],

$$C_{\mathbf{q}} = \pi^{3/2}V_R^2\sigma_R^3 \exp\left(-\sigma_R^2 q^2/4\right), \quad (11)$$

where V_R is the potential amplitude and σ_R denotes the radius of the autocorrelation function of the laser.

In our model, with the same atom densities and hence the same chemical potentials in the left and right parts of the system, there is no "charge" diffusion in the system. The spin polarization at the boundary between the left and right parts of the system is approximately treated to be fixed.

III. ANALYTICAL RESULTS

In this section, we analytically study the steady-state spin diffusion along the $\hat{\mathbf{x}}$ and $\hat{\mathbf{y}}$ directions in cold atoms with the atom-disorder scattering [Eq. (9)]. Both the situations with spin polarization perpendicular ($\mathbf{P}||\hat{\mathbf{z}}$) and parallel ($\mathbf{P}||\hat{\mathbf{x}}$) to the Zeeman field are analyzed.

In the steady state, the KSBEs are written as

$$(k_\zeta/m)\partial_\zeta\rho_{\mathbf{k}}(\mathbf{r}) + i[\Omega\sigma_x/2,\rho_{\mathbf{k}}(\mathbf{r})] + i[\alpha k_x\sigma_z/2,\rho_{\mathbf{k}}(\mathbf{r})] + \sum_{\mathbf{k}'} W_{\mathbf{k}\mathbf{k}'}[\rho_{\mathbf{k}}(\mathbf{r}) - \rho_{\mathbf{k}'}(\mathbf{r})] = 0, \quad (12)$$

where $W_{\mathbf{k}\mathbf{k}'} = 2\pi C_{\mathbf{k}-\mathbf{k}'}\delta(\varepsilon_{\mathbf{k}} - \varepsilon_{\mathbf{k}'})$. In the strong scattering regime with $l_\tau \ll l_\Omega, l_\alpha$ [i.e., $\langle|\Omega(\mathbf{k})|\rangle\tau_k \ll 1$], the steady-state diffusion lengths for different configurations are obtained and extended to the situation with moderate scattering strength ($l_\Omega \ll l_\tau \ll l_\alpha$ or $l_\alpha \ll l_\tau \ll l_\Omega$).

A. Spin diffusion along the $\hat{\mathbf{x}}$ direction

1. Analytical analysis

When the spin diffusion is along the $\hat{\mathbf{x}}$ direction, by taking the steady-state condition, the Legendre components of the azimuth-angle-averaged density matrix [Eq. (A2)] with respect to the zenith angle $\theta_{\mathbf{k}}$ are given by

$$\frac{k}{m}\frac{\partial}{\partial x}\left[\frac{l\bar{\rho}_k^{l-1}}{\sqrt{2l-1}} + \frac{(l+1)\bar{\rho}_k^{l+1}}{\sqrt{2l+3}}\right] + i\left[\frac{\Omega}{2}\sigma_x, \bar{\rho}_k^l\sqrt{2l+1}\right] + i\left[\frac{\alpha k}{2}\sigma_z, \frac{l\bar{\rho}_k^{l-1}}{\sqrt{2l-1}} + \frac{(l+1)\bar{\rho}_k^{l+1}}{\sqrt{2l+3}}\right] + \frac{\bar{\rho}_k^l}{\tau_{k,l}}\sqrt{2l+1} = 0, \quad (13)$$

in which the momentum relaxation time is denoted by

$$\tau_{k,l}^{-1} = \frac{m\sqrt{k}}{2\pi}\int_0^\pi C(\cos\theta)[1 - P_l(\cos\theta)]\sin\theta d\theta, \quad (14)$$

with $P_l(\cos\theta)$ being the Legendre function. By keeping both the zeroth and first orders ($l = 0,1$), the analytical solution for the spin polarization is obtained from Eq. (13) (refer to the Appendix). It is found that for the spin polarizations in both the transverse ($\hat{\mathbf{x}}$-T) and the longitudinal ($\hat{\mathbf{x}}$-L) configurations, the spin polarization is limited by one oscillation decay together with one single exponential decay, i.e.,

$$\mathbf{S}_\xi^x \approx A_\xi \exp\left(-x/L_o^x\right)\cos\left(x/l_o^x\right) + B_\xi \exp\left(-x/L_s^x\right), \quad (15)$$

with $\xi = t$ (transverse) or l (longitudinal). In Eq. (15), A_ξ and B_ξ are the amplitudes for the oscillation and single exponential decays, respectively, which are determined by the boundary condition; L_o^x and L_s^x are the decay lengths for the oscillation and single exponential decays, respectively; l_o^x is the oscillation length for the oscillation decay. The integral forms for L_s^x, L_o^x, and l_o^x are complicated [Eqs. (A9)–(A11) in the Appendix]. However, when the system is in the strong ($l_\tau \ll l_\Omega, l_\alpha$) and moderate ($l_\Omega \ll l_\tau \ll l_\alpha$ or $l_\alpha \ll l_\tau \ll l_\Omega$) scattering regimes, it is found that the analytical results can be reduced to simple forms, which can describe the behavior of the spin diffusion quite well (Sec. IV).

Specifically, for the oscillation decay,

$$L_o^x \approx \begin{cases} 2l_\tau/\sqrt{3}, & \text{when} \quad l_\Omega \ll l_\tau \ll l_\alpha, \\ \sqrt{2}l_\tau l_\Omega/(\sqrt{3}l_\alpha), & \text{when} \quad l_\alpha \ll l_\tau \ll l_\Omega, \\ \sqrt{2l_\tau l_\Omega/\sqrt{3}}, & \text{when} \quad l_\tau \ll l_\alpha \text{ and } l_\tau \ll l_\Omega. \end{cases} \quad (16)$$

The corresponding oscillation length,

$$l_o^x \approx \begin{cases} l_\Omega, & \text{when} \quad l_\Omega \ll l_\tau \ll l_\alpha, \\ l_\alpha, & \text{when} \quad l_\alpha \ll l_\tau \ll l_\Omega, \\ \sqrt{2l_\tau l_\Omega/\sqrt{3}}, & \text{when} \quad l_\tau \ll l_\alpha \text{ and } l_\tau \ll l_\Omega. \end{cases} \quad (17)$$

From Eq. (17), one further notes that l_Ω and l_α correspond to the spacial oscillation length due the Zeeman and spin-orbit coupled fields. Because of this, we refer to l_Ω and l_α as Zeeman and SOC oscillation lengths, respectively. For the single exponential decay, the diffusion length reads

$$L_s^x \approx \begin{cases} l_\tau l_\alpha/(\sqrt{3}l_\Omega), & \text{when} \quad l_\Omega \ll l_\tau \ll l_\alpha, \\ l_\tau l_\Omega/(\sqrt{3}l_\alpha), & \text{when} \quad l_\alpha \ll l_\tau \ll l_\Omega, \\ l_\alpha, & \text{when} \quad l_\tau \ll l_\alpha \text{ and } l_\tau \ll l_\Omega. \end{cases} \quad (18)$$

From these simple dependencies of the spin-diffusion length on the mean free path, the Zeeman oscillation length and the SOC oscillation length, the behavior of the steady-state spin polarization shown in Eq. (15) can be further simplified. It can be demonstrated that when $L_o^x \approx L_s^x$, $A_\xi \approx B_\xi$. Specifically, only when $L_o^x \approx L_s^x$, both the oscillation decay and single exponential decay are important, but with similar decay length. Otherwise, the spin polarization can be approximately reduced to one oscillation or single exponential decay, which depends on its amplitude in the spin polarization. In different regimes, the different behaviors for the steady-state spin polarization are analyzed as follows. In the Zeeman-field (SOC)-dominated moderate scattering regime with $l_\Omega \ll l_\tau \ll l_\alpha$ ($l_\alpha \ll l_\tau \ll l_\Omega$), the condition $L_o^x \approx L_s^x$ is never satisfied. Accordingly, when $l_\Omega \ll l_\tau \ll l_\alpha$ ($l_\alpha \ll l_\tau \ll l_\Omega$), the steady-state spin polarization is approximated by an oscillation and single exponential (single exponential and oscillation) decay for the transverse and longitudinal situations, respectively. In the

strong scattering regime ($l_\tau \ll l_\alpha, l_\Omega$), when $L_o^x \approx L_s^x$, one obtains

$$l_{\tau,x}^c \approx \sqrt{3} l_\alpha^2/(2l_\Omega), \tag{19}$$

which is referred to as the crossover length between the relatively strong and strong scattering regimes. Accordingly, when $l_\tau \gg l_{\tau,x}^c$ ($l_\tau \ll l_{\tau,x}^c$), the steady-state spin polarization is approximated by a single exponential and oscillation (oscillation and single exponential) decay in the transverse and longitudinal situations, respectively.

Based on the above analysis, we summarize the behaviors of the steady-state spin polarization and the spin-diffusion lengths in Table I for the two specific configurations $\hat{\mathbf{x}}$-T and $\hat{\mathbf{x}}$-L in different regimes. As shown in the table, the system is divided into five regimes: I, weak scattering regime ($l_\tau \gg l_\Omega, l_\alpha$); II, Zeeman field-dominated moderate scattering regime ($l_\Omega \ll l_\tau \ll l_\alpha$); III, SOC-dominated moderate scattering regime ($l_\alpha \ll l_\tau \ll l_\Omega$); IV, relatively strong scattering regime ($l_{\tau,x}^c \ll l_\tau \ll l_\alpha, l_\Omega$); V, strong scattering regime ($l_\tau \ll l_\alpha, l_\Omega, l_{\tau,x}^c$). In different regimes, it can be seen that the dependencies of the spin-diffusion length on the scattering strength, the Zeeman field, and SOC strength are very rich. Specifically, in the Zeeman field- (SOC-) dominated moderate scattering regime with $l_\Omega \ll l_\tau \ll l_\alpha$ ($l_\alpha \ll l_\tau \ll l_\Omega$), the longitudinal (longitudinal and transverse) spin diffusion is enhanced by the Zeeman field (SOC), whereas in the relatively strong (strong) scattering regime ($l_\tau \ll l_\alpha, l_\Omega$), the transverse (longitudinal) spin diffusion is determined by only the SOC oscillation length, but irrelevant to the Zeeman field with $l_\tau \gg l_{\tau,x}^c$ ($l_\tau \ll l_{\tau,x}^c$). The rich behaviors of the spin diffusions in different regimes are hard to understand in the framework of the previous simple drift-diffusion model [49–54] or the direct inhomogeneous broadening [Eqs. (2) and (3)] picture [45–48,55] in the literature. In the simple drift-diffusion model, there are only two rather than *five* regimes: the strong scattering regime with $l_s \propto 1/(m|\alpha|)$ and the weak scattering regime with $l_s \propto k\sqrt{\tau_k}/m$. In the direct inhomogeneous broadening picture, from Eq. (2), the Zeeman field (SOC) can (cannot) provide the inhomogeneous broadening. Hence, it seems that the spin diffusion can be suppressed by the Zeeman field, but irrelevant to the SOC. Below, we extend our previous inhomogeneous broadenings [Eqs. (2) and (3)] to the effective ones. We show that, based on the *effective* inhomogeneous broadening, apart from regime IV, the above anomalous behaviors of the spin diffusion can be understood from the view point of the helix representation [31,40]. In the helix space, apart from the spin-conserving scattering (the fifth term in the left-hand side of Eq. (A6) in our previous work [31]), additional terms arise including the helix spin-flip scattering (the sixth term in the left-hand side of Eq. (A6) in Ref. [31]) and helix coherence term (the last term in the left-hand side of Eq. (A6) in Ref. [31]).

2. *Comprehensive picture for regimes II and V*

When the system is in regime II, the Zeeman field-dominated moderate scattering regime ($l_\Omega \ll l_\tau \ll l_\alpha$), or regime V, the strong scattering regime ($l_\tau \ll l_\alpha, l_\Omega \ll l_{\tau,x}^c$), the condition $l_\Omega \ll l_\alpha$ is satisfied. Therefore, both the transverse and the longitudinal spin diffusions can be understood in the limit with strong Zeeman and weak spin-orbit-coupled fields. In this situation, the effective inhomogeneous broadening field is given by

$$\begin{aligned}\boldsymbol{\omega}_{\rm eff}^x(\mathbf{k}) &= (m/k_x)\sqrt{\Omega^2 + \alpha^2 k_x^2}\,\hat{\mathbf{x}}' \\ &\approx [m\Omega/k_x + m\alpha^2 k_x/(2\Omega)]\hat{\mathbf{x}}',\end{aligned} \tag{20}$$

with $\hat{\mathbf{x}}' = \frac{1}{\sqrt{1+(\alpha k_x/\Omega)^2}}\hat{\mathbf{x}} + \frac{\alpha k_x/\Omega}{\sqrt{1+(\alpha k_x/\Omega)^2}}\hat{\mathbf{z}}$ being nearly parallel to $\hat{\mathbf{x}}$. Under this effective field, the behaviors of the spin precession in the spacial domain for the transverse and longitudinal spin diffusions can be obtained, as schematically shown in Fig. 1. In this figure, for the transverse spin diffusion, the spin polarization is perpendicular to the strong Zeeman field and hence $\boldsymbol{\omega}_{\rm eff}^x(\mathbf{k})$ approximately. During the scattering, the spin vectors rotate around the effective inhomogeneous broadening field $\boldsymbol{\omega}_{\rm eff}^x(\mathbf{k})$ fast. Moreover, the scattering can also influence the spin diffusion. In the helix space, as mentioned above, apart from the original spin-conserving scattering, there exist the helix spin-flip scattering and helix coherence processes. However, with the helix spin-flip rate $\alpha^2 k^2/(\Omega^2\tau_k) \ll 1/\tau_k$ and helix coherence rate $\alpha k/(\Omega\tau_k) \ll 1/\tau_k$, when $\Omega \gg \alpha k$, both the helix spin-flip scattering and helix coherence can be neglected. In this situation, the effective inhomogeneous broadening together with the spin-conserving scattering determines the behavior of the spin diffusion. We refer to this picture as the *modified* inhomogeneous broadening picture. For the longitudinal situation, the spin polarization is nearly parallel to $\boldsymbol{\omega}_{\rm eff}^x(\mathbf{k})$, and hence the effective inhomogeneous broadening cannot cause the spin precession effectively. In this situation, the spin diffusion can be understood from the drift-diffusion model [49–54] modified as follows. The diffusion length $l_s = \sqrt{D\tau_s(\mathbf{k})}$ in which $D = v_F^2\tau_k/3$ is the diffusion coefficient, with v_F being the Fermi velocity. The SRT is analyzed in the helix space. First of all, for the longitudinal situation here, the helix coherence term has no contribution to the spin relaxation. In this situation, there are two channels influencing the spin relaxation: (i) the effective inhomogeneous broadening

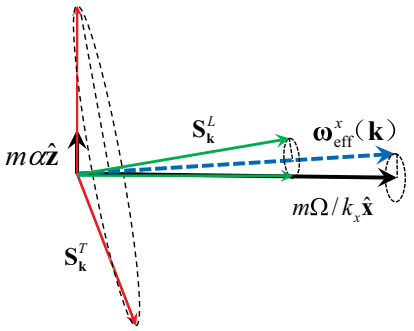

FIG. 1. (Color online) Schematic for the spin precession around the effective inhomogeneous broadening field $\boldsymbol{\omega}_{\rm eff}^x(\mathbf{k})$ [Eq. (20)] in the transverse ($\mathbf{S}_{\mathbf{k}}^T$) and longitudinal ($\mathbf{S}_{\mathbf{k}}^L$) spin diffusions. With the strong Zeeman and weak spin-orbit-coupled fields, for the transverse (longitudinal) situation, the spin vector $\mathbf{S}_{\mathbf{k}}^T$ ($\mathbf{S}_{\mathbf{k}}^L$) is perpendicular (parallel) to $\boldsymbol{\omega}_{\rm eff}^x(\mathbf{k})$ approximately. Therefore, the inhomogeneous broadening field can (cannot) cause efficient spin precession in the transverse (longitudinal) spin diffusion.

together with the spin-conserving scattering; (ii) the helix spin-flip scattering [31,40]. In the strong scattering regime, both channels (i) and (ii) are important for the spin relaxation, in which $\tau_s(\mathbf{k})$ remains the SRT in the conventional DP mechanism [29,30,32,45]. In the moderate scattering regime, channel (ii) is dominant for the spin relaxation, and hence $\tau_s(\mathbf{k})$ is replaced by the helix spin-flip rates determined in the helix space [31,40]. We refer to the above pictures as *modified* drift-diffusion model. Accordingly, in the moderate scattering regime, the dependence of the helix spin-flip rate on the scattering strength, the Zeeman field and SOC strength disclosed in our previous works [31,39,40] can also influence the spin diffusion.

Specifically, in the Zeeman field-dominated moderate scattering regime ($l_\Omega \ll l_\tau \ll l_\alpha$), i.e., regime II, the Zeeman oscillation length is the shortest length scale in the spin diffusion, which determines the behavior of spin precession in the spacial domain during the scattering. When the spin polarization is perpendicular to the Zeeman field (transverse configuration), the spin vector approximately precesses around $m\Omega/k_x\hat{\mathbf{x}}'$, leading to the spacial oscillations with the period proportional to $\langle|k_x|\rangle/(m\Omega)$ [$l_o^x \approx l_\Omega$ in Eq. (17)]. Moreover, due to the fast spacial oscillations with the strong Zeeman field, the spin memory is lost during one spin-conserving scattering, with the diffusion length being approximately the mean free path ($L_T^x \approx 2l_\tau/\sqrt{3}$ in Table I). When the spin polarization is parallel to the Zeeman field (longitudinal configuration), the effective inhomogeneous broadening $\boldsymbol{\omega}_{\rm eff}^x(\mathbf{k})$ cannot cause spin precession efficiently and the steady-state spin polarization decays without any oscillation. The spin diffusion can be understood from the modified drift-diffusion model [49–54]. Specifically, the helix spin-flip rate is calculated to be $\alpha^2k^2/(2\Omega^2\tau_k)$ in the moderate scattering situation [31,39,40]. Accordingly, the spin-diffusion length in the modified drift-diffusion model is given by $l_s \approx \sqrt{2}l_\tau l_\alpha/(\sqrt{3}l_\Omega)$, which is consistent with our model shown as $L_L^x \approx l_\tau l_\alpha/(\sqrt{3}l_\Omega)$ in Table I. Specifically, one notes that due to the suppression of the spin relaxation by the Zeeman field, the longitudinal spin-diffusion length is enhanced by the Zeeman field.

In regime V, the strong scattering regime ($l_\tau \ll l_\alpha, l_\Omega, l_{\tau,x}^c$), we consider a limit situation with the Zeeman field much stronger than the spin-orbit-coupled one ($l_\tau \ll l_\alpha, l_\Omega \ll l_{\tau,x}^c$). The effective inhomogeneous broadening is given by Eq. (20). For the transverse spin diffusion, because the inhomogeneous broadening given by the Zeeman field is dominant, the spin-diffusion length is suppressed by the Zeeman field, but less influenced by the SOC. Moreover, during the diffusion, the atoms experience several spin-conserving scatterings, which suppress the spin diffusion. Accordingly, we obtain a reasonable picture to understand $L_L^x \approx \sqrt{2l_\tau l_\Omega/\sqrt{3}}$ in Table I. For the longitudinal spin diffusion, the inhomogeneous broadening cannot cause the spin precession efficiently, with the steady-state spin polarization showing single exponential decay. Hence, the modified drift-diffusion model can be used [49–54]. With the SRT in the strong scattering regime $\tau_s(\mathbf{k}) \approx 2/(\alpha^2k^2\tau_k)$ [31,39,40], one obtains the spin-diffusion length $l_s \approx \sqrt{2}l_\alpha/\sqrt{3}$ ($L_T^x \approx l_\alpha$ in Table I). Therefore, the longitudinal spin-diffusion length depends only on the SOC oscillation length [31,49–54].

3. *Comprehensive picture for regimes III and IV*

When the system lies in regime III, the SOC-dominated moderate scattering regime ($l_\alpha \ll l_\tau \ll l_\Omega$), and regime IV, the relatively strong scattering regime ($l_{\tau,x}^c \ll l_\tau \ll l_\alpha, l_\Omega$), the spin-orbit-coupled field is much stronger than the Zeeman one. In this situation, the effective inhomogeneous broadening field reads

$$\begin{aligned}\boldsymbol{\omega}_{\rm eff}'^x(\mathbf{k}) &= (m/k_x)\sqrt{\alpha^2k_x^2+\Omega^2}\,\hat{\mathbf{z}}' \\ &\approx \left[m\alpha + m\Omega^2/\left(2\alpha k_x^2\right)\right]\hat{\mathbf{z}}', \end{aligned} \tag{21}$$

where $\hat{\mathbf{z}}' = \frac{1}{\sqrt{1+[\Omega/(\alpha k_x)]^2}}\hat{\mathbf{z}} + \frac{\Omega/(\alpha k_x)}{\sqrt{1+[\Omega/(\alpha k_x)]^2}}\hat{\mathbf{x}}$ is parallel to $\hat{\mathbf{z}}$ approximately. The analysis is similar to the situation with strong Zeeman and weak spin-orbit-coupled fields. One obtains that for the transverse (longitudinal) spin diffusion, the spin polarization is nearly parallel (perpendicular) to $\boldsymbol{\omega}_{\rm eff}'^x(\mathbf{k})$, which cannot (can) cause efficient spin precession. These pictures are summarized in Fig. 2. Therefore, the behavior of the transverse spin diffusion can be understood from the modified drift-diffusion model [49–54], whereas the longitudinal spin diffusion can be analyzed from the features of the precession of the spin vectors around $\boldsymbol{\omega}_{\rm eff}'^x(\mathbf{k})$.

Specifically, in regime III, i.e., the SOC-dominated moderate scattering regime ($l_\alpha \ll l_\tau \ll l_\Omega$), in the transverse configuration, the modified drift-diffusion model is used to understand the spin diffusion [49–54]. In the helix representation, the helix spin-flip rate is proportional to $\Omega^2/(\alpha^2k^2\tau_k)$ approximately [31,39,40]. The corresponding spin-diffusion length is proportional to $l_\tau l_\Omega/l_\alpha$, which is consistent with $L_T^x \approx l_\tau l_\Omega/(\sqrt{3}l_\alpha)$ in Table I. Consequently, one observes that the spin relaxation is suppressed by the spin-orbit-coupled field, and the transverse spin-diffusion length is enhanced by the SOC. In the longitudinal configuration, with $m|\alpha| \gg m\Omega^2/(2|\alpha|k_x^2)$, the spin polarization evolves with oscillations

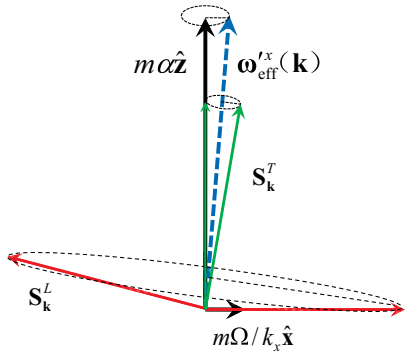

FIG. 2. (Color online) Schematic for the spin precession around the effective inhomogeneous broadening field $\boldsymbol{\omega}_{\rm eff}'^x(\mathbf{k})$ [Eq. (21)] in the transverse ($\mathbf{S}_\mathbf{k}^T$) and longitudinal ($\mathbf{S}_\mathbf{k}^L$) spin diffusions. With the weak Zeeman and strong spin-orbit-coupled fields, for the transverse (longitudinal) situation, the spin vector $\mathbf{S}_\mathbf{k}^T$ ($\mathbf{S}_\mathbf{k}^L$) is parallel (perpendicular) to $\boldsymbol{\omega}_{\rm eff}'^x(\mathbf{k})$ approximately. Therefore, the inhomogeneous broadening field cannot (can) cause efficient spin precession in the transverse (longitudinal) spin diffusion.

in the spacial domain, whose oscillation length is $l_o^x \approx l_\alpha$ [Eq. (17)]. Furthermore, only $m\Omega^2/(2\alpha k_x^2)\hat{\mathbf{z}}'$ in $\boldsymbol{\omega}'^x_{\rm eff}(\mathbf{k})$ can cause the inhomogeneous broadening. Therefore, it can be expected that the longitudinal spin diffusion length is inversely proportional (proportional) to the Zeeman field (SOC). Moreover, the spin-conserving scattering can suppress the spin diffusion in the modified inhomogeneous broadening picture. These analyses are consistent with $L_T^x \approx \sqrt{2}l_\tau l_\Omega/(\sqrt{3}l_\alpha)$ in Table I.

In regime IV, the relatively strong scattering regime ($l^c_{\tau,x} \ll l_\tau \ll l_\alpha, l_\Omega$), for the transverse spin diffusion, from the modified drift-diffusion model [49–54], $l_s \approx \sqrt{2}l_\alpha/\sqrt{3}$ ($L_T^x \approx l_\alpha$ in Table I). For the longitudinal spin diffusion, one expects that the modified inhomogeneous broadening picture can be applied. However, this picture fails to explain the behavior of the longitudinal spin diffusion. It can be seen from Eq. (21) that both the spin-orbit-coupled and Zeeman fields provide the inhomogeneous broadening [$m\Omega^2/(2\alpha k_x^2)\hat{\mathbf{z}}'$ in Eq. (21)]. By further considering that the spin diffusion is suppressed by the spin-conserving scattering, it is obtained that the spin-diffusion length is proportional to the SOC strength, but inversely proportional to the Zeeman field strength and scattering. However, in Table I, the longitudinal spin diffusion length $L_L^x \approx \sqrt{2l_\tau l_\Omega/\sqrt{3}}$ is irrelevant to the SOC strength. One further notices that regime IV lies in the crossover region between the moderate and the strong scattering regimes. When the scattering is relatively strong, the shortest length scale in the spin diffusion is the mean free path. However, there still exists strong competition between the effective inhomogeneous broadening and scattering, which makes the behavior of the spin diffusion complicated [47,54,55].

Finally, we address the behavior of the spin diffusion along the $\hat{\mathbf{x}}$ direction in the limit situation where the Zeeman field is zero. When $\Omega = 0$, l_Ω is infinite. The corresponding steady-state spin polarization shows very different behaviors compared to the situation with finite Zeeman field. In this situation, the transverse (longitudinal) spin diffusion length is infinite because $\boldsymbol{\omega}'^x_{\rm eff}(\mathbf{k})$ cannot cause inhomogeneous broadening [55]. Specifically, for the longitudinal situation, the spin polarization is perpendicular to the spin-orbit-coupled field, spin helix establishes with the oscillation length being l_α [30,55].

B. Spin diffusion along the $\hat{\mathbf{y}}$ direction

1. Analytical analysis

When the spin diffusion is along the $\hat{\mathbf{y}}$ direction, by taking the steady-state condition, the Fourier components of the azimuth-angle-averaged density matrix [Eq. (A2)] with respect to the zenith angle $\theta_{\mathbf{k}}$ are given by

$$\frac{\hbar k}{2im}\frac{\partial}{\partial y}\left(\tilde{\rho}_k^{l-1} - \tilde{\rho}_k^{l+1}\right) + i\left[\frac{\alpha k}{4}\sigma_z, \tilde{\rho}_k^{l+1} + \tilde{\rho}_k^{l-1}\right] + i\left[\frac{\Omega}{2}\sigma_x, \tilde{\rho}_k^{l}\right] + \frac{\tilde{\rho}_k^{l}}{\tilde{\tau}_{k,l}} = 0, \tag{22}$$

in which the momentum relaxation time is denoted by

$$\tilde{\tau}_{k,l}^{-1} = \frac{m\sqrt{k}}{2\pi}\int_0^\pi C(\cos\theta)[1-\cos(l\theta)]\sin\theta d\theta. \tag{23}$$

One notes that by choosing the Legendre and Fourier expansions of the density matrix for the spin diffusions along the $\hat{\mathbf{x}}$ and $\hat{\mathbf{y}}$ directions, the definitions for the momentum scattering time $\tau_{k,l}$ [Eq. (14)] and $\tilde{\tau}_{k,l}$ [Eq. (23)] are different. However, when $l = 1$, the two definitions are the same. By keeping both the zeroth and first orders ($l = 0,1$), the analytical solutions for the spin polarizations both perpendicular ($\hat{\mathbf{y}}$-T) and parallel ($\hat{\mathbf{y}}$-L) to the Zeeman field are obtained (refer to Sec. 2 of the Appendix).

When the spin polarization is perpendicular to the Zeeman field, in the moderate and strong scattering regimes, similar to the spin diffusion along the $\hat{\mathbf{x}}$ direction (Table I), the behaviors of the steady-state spin polarization are different with different scattering strengths. When the scattering is relatively weak, which satisfies $l_\tau > l^c_{\tau,y}$ with $l^c_{\tau,y} = \frac{4l_\alpha}{\sqrt{3}l_\Omega}\left(\frac{1}{l_\alpha^2} - \frac{8}{3l_\Omega^2}\right)^{-1/2}$, the steady-state spin polarization for $\mathbf{S}_T^y$ is limited by the bi-exponential decay, i.e.,

$$\mathbf{S}_T^y = P^+ \exp\left(-y/L_T^{y,+}\right) + P^- \exp\left(-y/L_T^{y,-}\right), \tag{24}$$

with $L_T^{y,\pm}$ being the diffusion length. It is further demonstrated that when $L_T^{y,+} \ll L_T^{y,-}$, $P^+ \ll P^-$ and hence the spin polarization [Eq. (24)] reduces to a single exponential decay with the decay length being $L_T^{y,-}$. Specifically, in the moderate scattering regime with $l_\alpha \ll l_\tau \ll l_\Omega$ ($l_\Omega \ll l_\tau \ll l_\alpha$), the condition $l_\tau > l^c_{\tau,y}$ is naturally (never) satisfied; in the strong scattering regime ($l^c_{\tau,y} < l_\tau \ll l_\alpha, l_\Omega$), it can be obtained that $l_\alpha \ll l_\Omega$ and hence $l^c_{\tau,y} \approx 4l_\alpha^2/(\sqrt{3}l_\Omega)$. Accordingly, when $l_\tau \gg l^c_{\tau,y}$, the diffusion length for $\mathbf{S}_T^y$ is written as

$$L_T^{y,-} \approx \begin{cases} \text{NA}, & \text{when} \quad l_\Omega \ll l_\tau \ll l_\alpha, \\ \sqrt{3}l_\tau l_\Omega/(2l_\alpha), & \text{when} \quad l_\alpha \ll l_\tau \ll l_\Omega, \\ \sqrt{3}l_\tau l_\Omega/(2l_\alpha), & \text{when} \quad l^c_{\tau,y} \ll l_\tau \ll l_\alpha, l_\Omega. \end{cases} \tag{25}$$

When the scattering is relatively strong, which satisfies $l_\tau < l^c_{\tau,y}$, the transverse spin polarization in the steady state is determined by the oscillation decay, i.e.,

$$\mathbf{S}_T^y = P_0 \exp\left(-y/L_T^y\right)\cos\left(y/l_T^y\right). \tag{26}$$

Here the decay length L_T^y and oscillation length l_T^y can be written as

$$L_T^y \approx \begin{cases} \sqrt{2}l_\tau, & \text{when} \quad l_\Omega \ll l_\tau \ll l_\alpha, \\ \text{NA}, & \text{when} \quad l_\alpha \ll l_\tau \ll l_\Omega, \\ \sqrt{\sqrt{3}l_\tau l_\Omega}, & \text{when} \quad l_\tau \ll l_\alpha, l_\Omega, l^c_{\tau,y}, \end{cases} \tag{27}$$

and

$$l_T^y \approx \begin{cases} \sqrt{3/2}l_\Omega, & \text{when} \quad l_\Omega \ll l_\tau \ll l_\alpha, \\ \text{NA}, & \text{when} \quad l_\alpha \ll l_\tau \ll l_\Omega, \\ \sqrt{\sqrt{3}l_\tau l_\Omega}, & \text{when} \quad l_\tau \ll l_\alpha, l_\Omega, l^c_{\tau,y}, \end{cases} \tag{28}$$

respectively.

When the spin polarization is parallel to the Zeeman field, it is found that the steady-state spin polarization is limited by the single exponential decay, i.e.,

$$\mathbf{S}_L^y = P_0 \exp\left(-y/L_L^y\right). \tag{29}$$

Here $L_L^y = l_\alpha\sqrt{l_\tau^2/(3l_\Omega^2)+1}$ is the decay length for $\mathbf{S}_L^y$. In the moderate and strong scattering regimes,

$$L_L^y \approx \begin{cases} l_\tau l_\alpha/(\sqrt{3}l_\Omega), & \text{when} \quad l_\Omega \ll l_\tau \ll l_\alpha, \\ l_\alpha, & \text{when} \quad l_\alpha \ll l_\tau \ll l_\Omega, \\ l_\alpha, & \text{when} \quad l_\tau \ll l_\Omega \text{ and } l_\tau \ll l_\alpha. \end{cases} \tag{30}$$

Based on the above results, in different regimes, the behaviors of the steady-state spin polarization and diffusion lengths are summarized in Table II for the two specific configurations $\hat{\mathbf{y}}$-T and $\hat{\mathbf{y}}$-L.

From Table II, it can be seen that the spin diffusion along the $\hat{\mathbf{y}}$ direction is divided into five regimes similar to those of the spin diffusion along the $\hat{\mathbf{x}}$ direction. The anomalous behaviors for the spin diffusion along the $\hat{\mathbf{x}}$ direction also exist here. Nevertheless, new features arise in the spin diffusion along the $\hat{\mathbf{y}}$ direction. It is shown in Table II that in regimes III, IV, and V, the longitudinal spin-diffusion length is only determined by the SOC oscillation length, but irrelevant to the scattering. This *robustness* to the scattering for the spin diffusion in a wide range is further revealed in the scattering dependence of the spin diffusion (Sec. IV A). Below it is found that, based on the modified drift-diffusion model and modified inhomogeneous broadening picture, apart from regime IV, all the features in different regimes can be obtained.

2. Comprehensive picture for regimes II and V

We first analyze regime II, the Zeeman field-dominated moderate scattering regime ($l_\Omega \ll l_\tau \ll l_\alpha$), and regime V, the strong scattering regime ($l_\tau \ll l_\alpha, l_\Omega \ll l_{\tau,y}^c$). In these two regimes, with strong Zeeman and weak spin-orbit coupled fields, the effective inhomogeneous broadening field is written as

$$\begin{aligned} \boldsymbol{\omega}_{\text{eff}}^y(\mathbf{k}) &= (m/k_y)\sqrt{\Omega^2+\alpha^2k_x^2}\,\hat{\mathbf{x}}' \\ &\approx \left[m\Omega/k_y + m\alpha^2k_x^2/(2\Omega k_y)\right]\hat{\mathbf{x}}', \end{aligned} \tag{31}$$

with $\hat{\mathbf{x}}'$ nearly parallel to $\hat{\mathbf{x}}$. In regime II, i.e., the Zeeman field-dominated moderate scattering regime ($l_\Omega \ll l_\tau \ll l_\alpha$), when the spin polarization is perpendicular to the Zeeman field (transverse configuration), in the spacial domain, the spin vectors precess approximately around $(m\Omega/k_y)\hat{\mathbf{x}}'$, which causes spacial oscillations whose period is proportional to $\langle|k_y|\rangle/(m\Omega)$ [$l_T^y \approx \sqrt{3/2}l_\Omega$ in Eq. (28)]. Moreover, due to the fast spacial oscillations, the spin memory is lost during one scattering, and hence the spin diffusion length is the mean free path approximately ($L_T^y \approx \sqrt{2}l_\tau$ in Table II). When the spin polarization is parallel to the Zeeman field (longitudinal configuration), the effective inhomogeneous broadening field $\boldsymbol{\omega}_{\text{eff}}^y(\mathbf{k})$ cannot cause spin precession efficiently and the steady-state spin polarization decays without any oscillation. From the modified drift-diffusion model [49–54], as calculated in Sec. III A, $l_s \approx \sqrt{2}l_\tau l_\alpha/(\sqrt{3}l_\Omega)$ [$L_L^y \approx l_\tau l_\alpha/(\sqrt{3}l_\Omega)$ in Table II].

In regime V, i.e., the strong scattering regime ($l_\tau \ll l_\alpha, l_\Omega, l_{\tau,y}^c$), we analyze the limit situation with strong Zeeman and weak spin-orbit coupled fields ($l_\tau \ll l_\alpha, l_\Omega \ll l_{\tau,y}^c$). For the transverse spin diffusion, the inhomogeneous broadening is dominantly determined by the Zeeman field [Eq. (31)]. Hence, the transverse spin-diffusion length is suppressed by the Zeeman field, but less influenced by the SOC. Furthermore, during the diffusion, the spin-conserving scattering suppresses the spin diffusion ($L_L^y \approx \sqrt{\sqrt{3}l_\tau l_\Omega}$ in Table II). For the longitudinal spin diffusion, the inhomogeneous broadening cannot cause the spin precession efficiently (single exponential decay). According to the modified drift-diffusion model, the spin diffusion length depends only on the SOC oscillation length ($L_T^y \approx l_\alpha$ in Table I).

3. Comprehensive picture for regimes III and IV

We then analyze regime III, SOC-dominated moderate scattering regime ($l_\alpha \ll l_\tau \ll l_\Omega$), and regime IV, relatively strong scattering regime ($l_{\tau,y}^c \ll l_\tau \ll l_\alpha, l_\Omega$). With weak Zeeman and strong spin-orbit-coupled fields, the effective inhomogeneous broadening field reads

$$\begin{aligned} \boldsymbol{\omega}'^y_{\text{eff}}(\mathbf{k}) &= (m/k_y)\sqrt{\alpha^2k_x^2+\Omega^2}\,\hat{\mathbf{z}}' \\ &\approx [m\alpha k_x/k_y + m\Omega^2/(2\alpha k_x k_y)]\hat{\mathbf{z}}', \end{aligned} \tag{32}$$

where $\hat{\mathbf{z}}'$ is parallel to $\hat{\mathbf{z}}$ approximately. In the SOC-dominated moderate scattering regime (regime III with $l_\alpha \ll l_\tau \ll l_\Omega$), in the transverse configuration, the spin polarization is nearly parallel to $\boldsymbol{\omega}'^y_{\text{eff}}(\mathbf{k})$. Therefore, the effective inhomogeneous broadening cannot cause the spin precession effectively (single exponential decay). From the modified drift-diffusion model, the diffusion length is proportional to $l_\Omega l_\tau/l_\alpha$, which is consistent with $L_y^T \approx \sqrt{3}l_\Omega l_\tau/(2l_\alpha)$ in Table II. In the longitudinal configuration, the steady-state spin polarization is perpendicular to $\boldsymbol{\omega}'^y_{\text{eff}}(\mathbf{k})$ approximately. One notes that in $\boldsymbol{\omega}'^y_{\text{eff}}(\mathbf{k})$, the spin-orbit-coupled field $(m\alpha k_x/k_y)\hat{\mathbf{z}}'$ provides the dominant inhomogeneous broadening. Moreover, this inhomogeneous broadening not only depends on k_y but also k_x, which can be more efficient than the one depending only on k_x or k_y. Due to this efficient inhomogeneous broadening, the steady-state spin polarization decays due to the interference without oscillation. Moreover, the spin memory can be lost in the scale of SOC oscillation length, which cannot persist in the mean free path ($L_L^y \approx l_\alpha$ in Table II). This is different from the transverse spin diffusion in the Zeeman field-dominated moderate scattering regime ($l_\Omega \ll l_\tau \ll l_\alpha$).

In the relatively strong scattering regime (regime IV with $l_{\tau,y}^c \ll l_\tau \ll l_\alpha, l_\Omega$), from Table II, one observes that the behaviors for both the transverse and longitudinal spin diffusions are similar to the ones in regime III, i.e., the SOC-dominated moderate scattering regime ($l_\alpha \ll l_\tau \ll l_\Omega$). We address that this behavior is hard to understand from both the modified drift-diffusion model and the modified inhomogeneous broadening picture. For the transverse spin diffusion, the spin polarization is nearly parallel to $(m\alpha k_x/k_y)\hat{\mathbf{z}}'$, and hence the spin-diffusion length is $\sqrt{2}l_\alpha/\sqrt{3}$ from the modified drift-diffusion model. For the longitudinal spin diffusion, the spin polarization is perpendicular to the inhomogeneous broadening field $(m\alpha k_x/k_y)\hat{\mathbf{z}}'$ approximately, and hence the SOC can suppress the spin diffusion. Moreover, the spin-conserving scattering can suppress the longitudinal spin diffusion. From this analysis, the longitudinal spin-diffusion length is suppressed by the SOC strength and scattering, but irrelevant to the Zeeman field (modified inhomogeneous broadening picture). However, the pictures above fail to explain the transverse and

longitudinal spin diffusion lengths for regime IV in Table II with $L_T^y \approx \sqrt{3} l_\tau l_\Omega/(2l_\alpha)$ and $L_L^y \approx l_\alpha$. This is because for the transverse situation, although the modified drift diffusion model can explain the spin diffusion along the $\hat{\mathbf{x}}$ direction, it is too rough to consider the anisotropy between the diffusions along the $\hat{\mathbf{x}}$ and $\hat{\mathbf{y}}$ directions in the relatively strong scattering regime. This was first pointed out by Zhang and Wu in the study of the spin diffusion in graphene [54]. For the longitudinal spin diffusion, when the scattering is strong, the shortest length scale in the spin diffusion is the mean free path. In this situation, there exists strong competition between the effective inhomogeneous broadening and scattering, which makes the behavior of the spin diffusion complicated [47,54,55].

Finally, we emphasize that from Table II, for the transverse spin diffusion along the $\hat{\mathbf{y}}$ direction, in regimes III, IV, and V, the spin-diffusion lengths are irrelevant to the scattering. Therefore, with weak Zeeman and strong spin-orbit-coupled fields ($l_\alpha \ll l_\Omega$), a specific situation can be realized where the spin-diffusion length is robust against the scattering except with the extremely weak scattering. It is noted that in the strong scattering regime, this feature was predicted in the simple drift-diffusion model [49–53] and was also revealed in graphene by the KSBE approach [54]. In this work, we have further extended it into the weak scattering regime.

IV. NUMERICAL RESULTS

In the numerical calculation, the KSBEs are solved by employing the double-side boundary conditions [47],

$$\rho_{\mathbf{k}}(\zeta = 0,t) = \frac{f_{\mathbf{k}\uparrow} + f_{\mathbf{k}\downarrow}}{2} + \frac{f_{\mathbf{k}\uparrow} - f_{\mathbf{k}\downarrow}}{2}\boldsymbol{\sigma}\cdot\hat{\mathbf{n}},\ k_\zeta > 0,$$
$$\rho_{\mathbf{k}}(\zeta = L,t) = f^0_{\mathbf{k}},\quad k_\zeta < 0, \tag{33}$$

where $f_{\mathbf{k}\sigma} = \{\exp[(\varepsilon_{\mathbf{k}} - \mu_\sigma)/(k_B T)] + 1\}^{-1}$ is the Fermi distribution function at temperature T, with $\mu_{\uparrow,\downarrow}$ standing for the chemical potentials determined by the atom density $n_a = \sum_{\mathbf{k}} \mathrm{Tr}[\rho_{\mathbf{k}}]$ and the spin polarization $P(0)$ in the left part of the system; $\hat{\mathbf{n}}$ denotes the spin polarization direction; $f^0_{\mathbf{k}}$ is the Fermi distribution at equilibrium. When the system evolves to the steady state, one obtains the diffusion length from the spatial evolution of the spin polarization $P(\zeta) = \sum_{\mathbf{k}} \mathrm{Tr}[\rho_{\mathbf{k}}(\zeta)\boldsymbol{\sigma}\cdot\hat{\mathbf{n}}]/n_a$.

Within the experimental feasibility by referring to the experiment by Wang *et al.* [26], the parameters are chosen as follows. The lowest two magnetic sublevels $|9/2,9/2\rangle$ and $|9/2,7/2\rangle$ are coupled by a pair of Raman beams with wavelength $\lambda = 773$ nm and the frequency difference $\omega/(2\pi) = 10.27$ MHz. The Raman detuning $\delta = \omega_z - \omega$ is set to be zero by choosing the Zeeman shift $\omega_z/(2\pi) = 10.27$ MHz. The recoil momentum and energy are set to be $k_r = k_0/10$, with $k_0 = 2\pi/\lambda$, and hence $E_r = k_r^2/(2m) = 2\pi \times 83.4$ Hz. In our study, the SOC strength varies from $0.5\alpha_0$ to $6\alpha_0$ with $\alpha_0 = -2k_r/m$. The strengths of the Zeeman field Ω vary from $10E_r$ to $450E_r$. Furthermore, the Fermi momentum is set to be $k_F = 30k_r$ [26]. It is noted that with these parameters, the condition that the Zeeman and SOC energies are much smaller than the Fermi energy is satisfied.

Moreover, the temperature is set to $T = 0.3T_F$, with T_F being the corresponding Fermi temperature [26]. With these parameters, the thermal deBroglie wavelength $\Lambda_{dB} = h/\sqrt{2\pi m k_B T} \approx 0.26\mu$m. For the 3D isotropic speckle disorder, $V_R/k_B = 1250$ nK and $\sigma_R = 0.27\mu$m [34–36]. With these disorder parameters, the mean free path $l_\tau \approx 5\mu$m. In our study, the strength of the disorder strength V is tuned by the laser [34–38,44]. One notes that when $(V/V_R)^2 \gtrsim 20$, $l_\tau \lesssim \Lambda_{dB}$. According to the Ioffe-Regel condition for the Anderson localization [64,65], the Anderson localization may become relevant [34–36]. Nevertheless, in our study, to distinguish different regimes as well as compare with the analytical results in different regimes revealed in Sec. III, the numerical calculations are extended artificially to $(V/V_R)^2 \gg 20$. In reality, when the system enters into the localization regime when $(V/V_R)^2 \gtrsim 20$, the atoms with energy below the mobility edge becomes localized [34–36,65]. In this situation, no diffusion is permitted for these low-energy atoms. Even by considering the atoms with energy higher than the mobility edge, in the localization regime, the diffusion length can be expected to decrease with the increase of the disorder strength.

A. Scattering strength dependence

In this part, we study the scattering strength dependence of the steady-state spin diffusion of spin-orbit coupled ^{40}K gas in the 3D isotropic speckle disorder. The SOC strength is set to be α_0 and the spin polarization is chosen to be $P = 20\%$. For the spin diffusion along the $\hat{\mathbf{x}}$ direction ($\hat{\mathbf{y}}$ direction), both the transverse and longitudinal spin-diffusion lengths L_T^x and L_L^x (L_T^y and L_L^y) are shown in Figs. 3(a) and 3(b) [Figs. 3(c) and 3(d)].

We first analyze the spin diffusion along the $\hat{\mathbf{x}}$ direction [Figs. 3(a) and 3(b)]. For the transverse spin diffusion, it can be seen from Fig. 3(a) that whether the Zeeman field is strong with $\Omega = 450E_r$ (the blue dashed curve with squares) or weak with $\Omega = 10E_r$ (the red solid curve with circles), the transverse spin diffusion length L_T^x decreases with the increase of the disorder strength. The underlying physics can be understood as follows. We first calculate the characteristic lengths for the system defined in Sec. III: the SOC oscillation length $l_\alpha \approx 0.6\ \mu$m; the Zeeman oscillation length $l_\Omega \approx 0.1\ \mu$m (4 μm) for $\Omega = 450E_r$ ($10E_r$); when $\Omega = 450E_r$ ($10E_r$), the crossover length between the relatively strong and strong scattering regimes $l^c_{\tau,x} \approx \sqrt{3} l_\alpha^2/(2l_\Omega) \approx 3\ \mu$m (0.08 μm), i.e., $(V/V_R)_c^2 \approx 2$ [$(V/V_R)_c^2 \approx 65$]. Furthermore, it is calculated that when $l_\tau \approx l_\alpha$, $(V/V_R)^2 \approx 8$; when $l_\tau \approx l_\Omega$, $(V/V_R)^2 \approx 50$ [$(V/V_R)^2 \approx 1$] for $\Omega = 450E_r$ ($10E_r$). Accordingly, with the increase of the disorder strength, the system experiences several regimes. For $\Omega = 450E_r$, the regimes are approximately divided into

$$\begin{aligned} &\mathrm{I}: l_\tau \gtrsim l_\Omega, l_\alpha, \quad \text{when} \quad (V/V_R)^2 \lesssim 8, \\ &\mathrm{II}: l_\Omega \lesssim l_\tau \lesssim l_\alpha, \quad \text{when} \quad 8 \lesssim (V/V_R)^2 \lesssim 50, \\ &\mathrm{V}: l_\tau \ll l_\Omega, l_\alpha, l^c_{\tau,x} \quad \text{when} \quad (V/V_R)^2 \gg 50, \end{aligned} \tag{34}$$

which are labeled by the blue roman numbers with the boundaries indicated by the blue crosses at the bottom frame of Fig. 3(b). Therefore, when $(V/V_R)^2 \lesssim 8$, the system is in regime I, and our calculation shows that the transverse diffusion length decreases with the increase of the disorder strength. When $8 \lesssim (V/V_R)^2 \lesssim 50$ [$(V/V_R)^2 \gg 50$], the system lies in

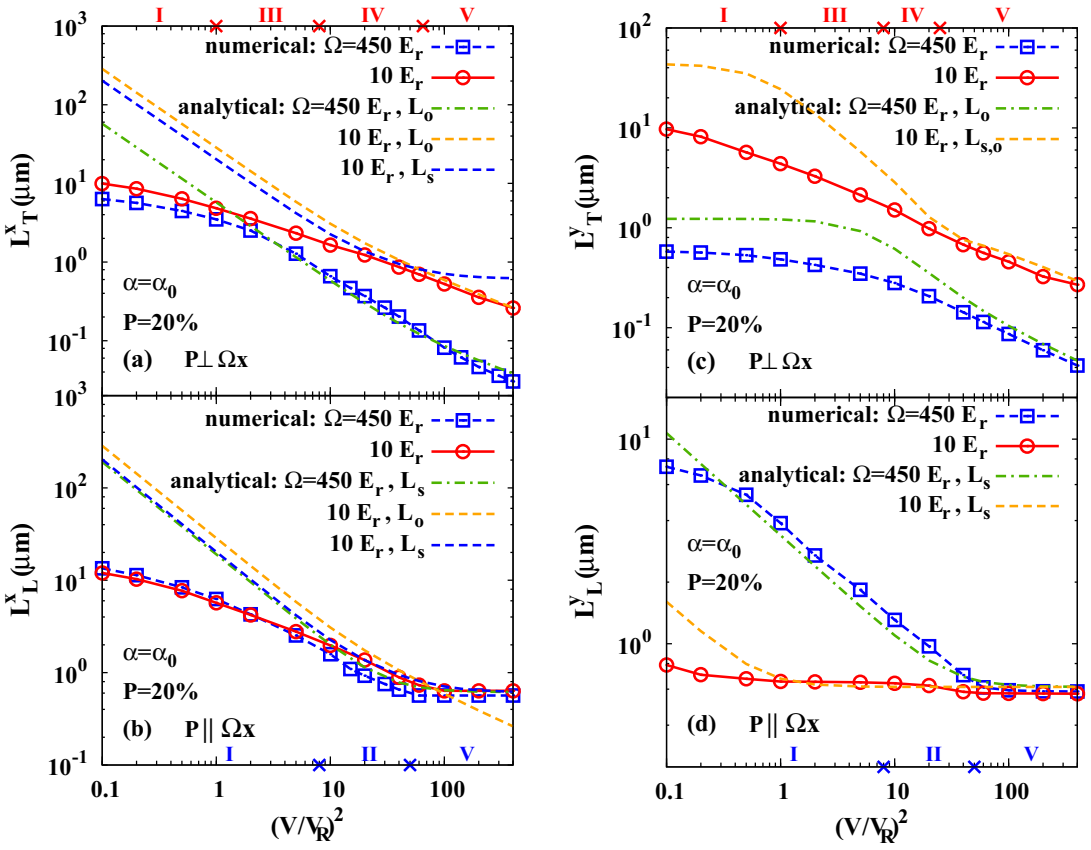

FIG. 3. (Color online) Scattering strength dependence of the steady-state spin diffusion of spin-orbit-coupled ^{40}K gas with the 3D isotropic speckle disorder. The SOC strength $\alpha = \alpha_0$ and the spin polarization $P = 20\%$. For the spin diffusion along the $\hat{\mathbf{x}}$ direction ($\hat{\mathbf{y}}$ direction), the transverse and longitudinal spin diffusion lengths L_T^x and L_L^x (L_T^y and L_L^y) are shown in Figs. 3(a) and 3(b) [Figs. 3(c) and 3(d)], respectively. Situations with strong ($\Omega = 450E_r$) and weak ($\Omega = 10E_r$) Zeeman fields are calculated both analytically and numerically. The blue (red) crosses on the frames indicate the boundaries between different regimes represented by the blue (red) roman numbers at the bottom (top) frame when $\Omega = 450E_r$ ($10E_r$). It is shown that the analytical calculations agree with the numerical ones in the relatively strong to strong scattering regime and crossover region between the relatively strong and moderate scattering regimes.

regime II (V), and from Table I, one comes to $L_T^x \approx 2l_\tau/\sqrt{3}$ ($L_T^x \approx \sqrt{2l_\tau l_\Omega/\sqrt{3}}$) with the steady-state spin polarization showing oscillation decay. Hence, the transverse spin-diffusion length decreases with the increase of the disorder strength. One notes that the corresponding results calculated from the analytical formula Eq. (A10) (the green dot-dashed curve) agree with the numerical ones in regimes II and V in Fig. 3(a). For $\Omega = 10E_r$, the regimes are approximately divided into

$$\begin{aligned} &\text{I}: l_\tau \gtrsim l_\Omega, l_\alpha, \quad \text{when} \quad (V/V_R)^2 \lesssim 1, \\ &\text{III}: l_\alpha \lesssim l_\tau \lesssim l_\Omega, \quad \text{when} \quad 1 \lesssim (V/V_R)^2 \lesssim 8, \\ &\text{IV}: l^c_{\tau,x} \lesssim l_\tau \lesssim l_\Omega, l_\alpha, \quad \text{when} \quad 8 \lesssim (V/V_R)^2 \lesssim 65, \\ &\text{V}: l_\tau \ll l_\Omega, l_\alpha, l^c_{\tau,x}, \quad \text{when} \quad (V/V_R)^2 \gg 65, \end{aligned} \tag{35}$$

which are shown by the red roman numbers with the boundaries indicated by the red crosses at the top frame of Fig. 3(a). Specifically, in regime I when $(V/V_R)^2 \lesssim 1$, it is shown that the transverse spin-diffusion length decreases with the increase of the scattering strength. In regime III [V] with $1 \lesssim (V/V_R)^2 \lesssim 8$ [$(V/V_R)^2 \gg 65$], from Table I, it is obtained that $L_T^x \approx l_\tau l_\Omega/(\sqrt{3}l_\alpha)$ ($L_T^x \approx \sqrt{2l_\tau l_\Omega/\sqrt{3}}$) with the steady-state spin polarization being single exponential (oscillation) decay. Hence, the transverse spin diffusion length decreases with the increase of disorder strength. One further notices that in Fig. 3(a), the result calculated from the analytical formula Eq. (A10) (the orange dashed curve) agrees with the numerical one in regime V.

For the longitudinal spin diffusion along the $\hat{\mathbf{x}}$ direction, it can be seen from Fig. 3(b) that whether the Zeeman field is strong ($450E_r$, blue dashed curve with squares) or weak ($10E_r$, red solid curve with circles), with the increase of the disorder strength, the spin-diffusion length decreases first and then becomes insensitive to the scattering. This can be understood as follows. With the increase of the disorder strength, the corresponding regimes can also be divided according to Eq. (34) [Eq. (35)] when $\Omega = 450E_r$ ($10E_r$). Specifically, when $(V/V_R)^2 \lesssim 8$ [$(V/V_R)^2 \lesssim 1$] for $\Omega = 450E_r$ [$10E_r$], the system is in regime I, with the longitudinal spin diffusion suppressed by the scattering. When $8 \lesssim (V/V_R)^2 \lesssim 50$ [$1 \lesssim (V/V_R)^2 \lesssim 8$] for $\Omega = 450E_r$ [$10E_r$], the system lies in regime II (III), and one comes to $L_L^x \approx l_\tau l_\alpha/(\sqrt{3}l_\Omega)$ [$L_L^x \approx \sqrt{2}l_\tau l_\Omega/(\sqrt{3}l_\alpha)$] with the steady-state spin polarization showing single exponential (oscillation) decay. When $(V/V_R)^2 \gg 50$ [$(V/V_R)^2 \gg 65$] for $\Omega = 450E_r$ [$10E_r$], the system lies in regime V, it is obtained that $L_L^x \approx l_\alpha$

(single exponential decay). Therefore, the longitudinal spin diffusion is suppressed first and then becomes insensitive to the scattering with the increase of the disorder strength. Also in Fig. 3(b), for $\Omega = 450E_r$, it is shown that the results calculated from the analytical formula Eq. (A9) (the green dot-dashed curve) agrees with the numerical one in both regimes II and V; for $\Omega = 10E_r$, the analytical results (the blue dashed curve) agree with the numerical ones in regime V.

We then turn to the spin diffusion along the $\hat{\mathbf{y}}$ direction [Figs. 3(c) and 3(d)]. For the transverse spin diffusion, it is shown in Fig. 3(c) that for both the strong ($450E_r$, blue dashed curve with squares) and the weak ($10E_r$, red solid curve with circles) Zeeman fields, the spin-diffusion length decreases with the increase of the disorder strength. It is calculated that for $\Omega = 450E_r$ [$10E_r$], $l^c_{\tau,y} \approx 8.3\mu$m [$0.2\mu$m], i.e., $(V/V_R)^2_c \approx 0.6$ [$(V/V_R)^2_c \approx 25$]. Accordingly, when the Zeeman field is strong ($\Omega = 450E_r$), one can divide the regimes according to Eq. (34). Specifically, when $(V/V_R)^2 \lesssim 8$, the transverse spin diffusion is calculated to be suppressed by the scattering. When $8 \lesssim (V/V_R)^2 \lesssim 50$ [$(V/V_R)^2 \gg 50$], one obtains from Table II that $L^y_T \approx \sqrt{2}l_\tau$ [$L^y_T \approx \sqrt{\sqrt{3}l_\Omega l_\tau}$], with the steady-state spin polarization showing oscillation decay. Therefore, with the increase of the scattering strength, the transverse spin diffusion is suppressed. When the Zeeman field is weak ($10E_r$), the regimes are approximately divided into

$$\begin{aligned} &\mathrm{I}: l_\tau \gtrsim l_\Omega, l_\alpha, \quad \text{when} \quad (V/V_R)^2 \lesssim 1, \\ &\mathrm{III}: l_\alpha \lesssim l_\tau \lesssim l_\Omega, \quad \text{when} \quad 1 \lesssim (V/V_R)^2 \lesssim 8, \\ &\mathrm{IV}: l^c_{\tau,y} \lesssim l_\tau \lesssim l_\Omega, l_\alpha, \quad \text{when} \quad 8 \lesssim (V/V_R)^2 \lesssim 25, \\ &\mathrm{V}: l_\tau \ll l_\Omega, l_\alpha, l^c_{\tau,y}, \quad \text{when} \quad (V/V_R)^2 \gg 25, \end{aligned} \tag{36}$$

which are labeled by the red roman numbers with the boundaries indicated by the red crosses at the top frame of Fig. 3(c). Specifically, when $(V/V_R)^2 \lesssim 1$, the transverse spin-diffusion length decreases with the increase of the disorder strength. When $1 \lesssim (V/V_R)^2 \lesssim 8$ [$(V/V_R)^2 \gg 25$], it is obtained from Table II that $L^y_T \approx \sqrt{3}l_\Omega l_\tau/(2l_\alpha)$ [$L^y_T \approx \sqrt{\sqrt{3}l_\Omega l_\tau}$], with the steady-state spin polarization being single exponential (oscillation) decay. Therefore, the transverse spin-diffusion length decreases with the increase of the disorder strength. Furthermore, it can be seen in Fig. 3(c) that the results calculated from the analytical formulas Eqs. (A19) and (A22) agree with the numerical ones in regime V.

For the longitudinal spin diffusion along the $\hat{\mathbf{y}}$ direction, it is shown in Fig. 3(d) that with the increase of the scattering strength, for both the strong ($450E_r$) and the weak ($10E_r$) Zeeman fields, the longitudinal spin-diffusion length is suppressed first and then becomes insensitive to the scattering. Specifically, when $\Omega = 10E_r$ ($l_\alpha \ll l_\Omega$), the longitudinal spin diffusion is robust against the scattering except with extremely weak scattering. Here, for the strong (weak) Zeeman field $\Omega = 450E_r$ [$10E_r$], the regimes are divided according to Eq. (34) [Eq. (36)]. For the strong Zeeman field ($450E_r$), when $(V/V_R)^2 \lesssim 8$, the longitudinal spin diffusion is suppressed by the scattering. When $8 < (V/V_R)^2 \lesssim 50$ [$(V/V_R)^2 \gg 50$], it is obtained from Table II that $L^y_L \approx l_\tau l_\alpha/(\sqrt{3}l_\Omega)$ [$L^y_L \approx l_\alpha$], with the steady-sate spin polarization being single exponential decay. Hence, the longitudinal spin-diffusion length decreases first and then become insensitive to the scattering with the increase of the disorder strength. For the weak Zeeman field ($10E_r$), when $(V/V_R)^2 \lesssim 1$, our calculation shows that the longitudinal spin-diffusion length decreases slowly with the increase of the disorder strength. When $(V/V_R)^2 \gtrsim 1$, one obtains from Table II that $L^y_L \approx l_\alpha$ (single exponential decay). Hence, the longitudinal spin-diffusion length is insensitive to the scattering in a wide range. Moreover, it is shown in Fig. 3(d) that the results calculated from the analytical formula Eq. (A15) agree with the numerical ones in both the moderate and strong scattering regimes. It is emphasized again here that notwithstanding the fact that the calculation is extended to the localization regime with $(V/V_R)^2 \gtrsim 20$, it is just for the sake of highlighting different regimes.

Finally, we address the specific features in the scattering strength dependence of the transverse and longitudinal spin diffusions along the $\hat{\mathbf{x}}$ and $\hat{\mathbf{y}}$ directions. Our calculations show that in the weak ($l_\tau \gtrsim l_\Omega, l_\alpha$) scattering regime (regime I), both the transverse and the longitudinal spin diffusions are suppressed by the scattering. In the strong scattering limit ($l_\tau \ll l_\Omega, l_\alpha, l^c_\tau$), the longitudinal spin diffusions along the $\hat{\mathbf{x}}$ and $\hat{\mathbf{y}}$ directions are insensitive to the scattering. Specifically, when $l_\alpha \ll l_\Omega$, the longitudinal spin diffusion along the $\hat{\mathbf{y}}$ direction is robust against the scattering except with extremely weak scattering. We emphasize that this robust spin diffusion cannot be obtained from the oversimplified drift-diffusion model, where $l_s = \sqrt{D\tau_s(\mathbf{k})}$, with $D = v_F^2\tau_k/3$ [49–54]. From the drift-diffusion model, in regime V with $\tau_s(\mathbf{k}) \propto \tau_k^{-1}$, one surely obtains that the spin-diffusion length is irrelevant to the scattering. However, in regimes I and II, i.e., the weak scattering regime defined in the conventional DP spin relaxation [39,41,45], $\tau_s(\mathbf{k}) \approx \tau_k$. Hence, it is obtained that $l_s \propto \tau_k$ with the spin-diffusion length suppressed by the scattering. One further notes that the experimental condition can be easily realized to observe this robust spin diffusion. On one hand, the spin diffusion is set to be along the $\hat{\mathbf{y}}$ direction with the initial spin polarization parallel to the Zeeman field; on the other hand, the Zeeman field is tuned to be much weaker than the spin-orbit coupled one by the laser field.

B. Zeeman field dependence

In this part, we address the Zeeman field dependence of the transverse and longitudinal spin diffusions along the $\hat{\mathbf{x}}$ [Fig. 4(a)] and $\hat{\mathbf{y}}$ directions [Fig. 4(b)]. The SOC strength is set to be α_0 and the spin polarization is chosen to be $P = 20\%$. Here we mainly address the specific features in the Zeeman field dependence when the system lies in the moderate and strong scattering regimes, which can be realized by setting $(V/V_R)^2 = 60$ and $(V/V_R)^2 = 10$, respectively.

We first focus on the case with $(V/V_R)^2 = 60$. When $(V/V_R)^2 = 60$, one observes from Figs. 4(a) and 4(b) that for the spin diffusion along both the $\hat{\mathbf{x}}$ and the $\hat{\mathbf{y}}$ directions, the transverse diffusion length decreases with the increase of the Zeeman field, as shown by the red solid curve with squares. This is because when $(V/V_R)^2 = 60$, for the spin diffusion along the $\hat{\mathbf{x}}$ direction ($\hat{\mathbf{y}}$ direction), $l_\tau \lesssim l_\alpha, l_\Omega, l^c_{\tau,x}$ ($l_\tau \lesssim l_\alpha, l_\Omega, l^c_{\tau,y}$) is satisfied. Hence, the system lies in regime V. Accordingly, for the transverse spin diffusion along the $\hat{\mathbf{x}}$ direction ($\hat{\mathbf{y}}$ direction), one obtains from Table I [Table II]

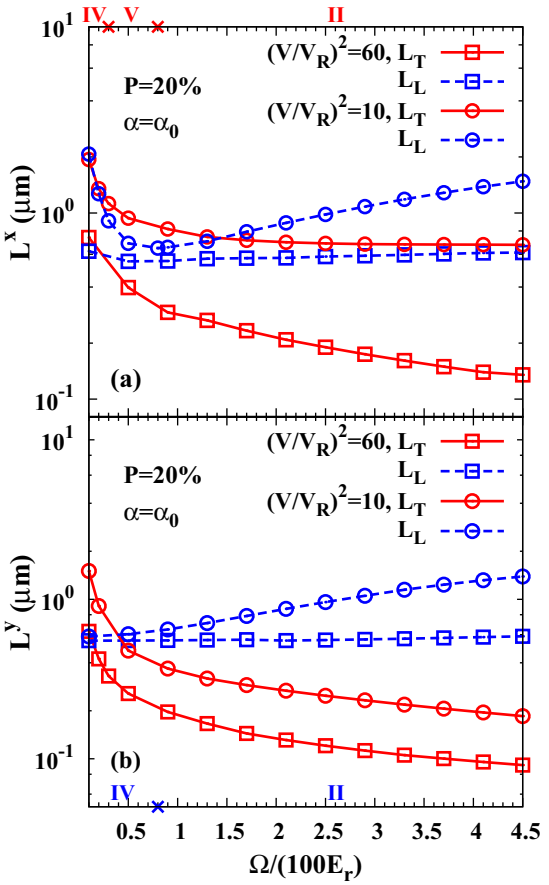

FIG. 4. (Color online) Zeeman field dependence of the transverse and longitudinal spin diffusions along the (a) $\hat{\mathbf{x}}$ and (b) $\hat{\mathbf{y}}$ directions. The SOC strength $\alpha = \alpha_0$ and the spin polarization $P = 20\%$. The situations with the scattering strengths $(V/V_R)^2 = 60$ (squares) and $(V/V_R)^2 = 10$ (circles) calculated numerically are presented. The green (blue) roman numbers at the top (bottom) frame represent the different regimes when $(V/V_R)^2 = 10$ for the spin diffusion along the $\hat{\mathbf{x}}$ direction ($\hat{\mathbf{y}}$ direction), with the boundaries indicated by the green (blue) crosses.

that $L_T^x \approx \sqrt{2l_\tau l_\Omega/\sqrt{3}}$ [$L_T^y \approx \sqrt{3}l_\Omega l_\tau/(2l_\alpha)$]. Therefore, with the increase of the Zeeman field, the transverse spin-diffusion length decreases. For the longitudinal spin diffusion, it is shown in Figs. 4(a) and 4(b) that whether the spin diffusion is along the $\hat{\mathbf{x}}$ direction or the $\hat{\mathbf{y}}$ direction, the spin-diffusion length is marginally influenced by the Zeeman field (blue dashed curve with squares). This anomalous behavior can be well understood from the analytical results in regime V. For the longitudinal spin diffusion along the $\hat{\mathbf{x}}$ direction ($\hat{\mathbf{y}}$ direction), it is obtained that $L_L^x \approx l_\alpha$ ($L_L^y \approx l_\alpha$). Accordingly, in regime V, the longitudinal spin diffusions along both the $\hat{\mathbf{x}}$ and the $\hat{\mathbf{y}}$ directions are marginally influenced by the Zeeman field. Based on the drift-diffusion model [49–54], it is emphasized that this unique feature arises from the insensitivity of diffusion coefficient and SRT to the Zeeman field in the strong scattering limit.

We then analyze the case with $(V/V_R)^2 = 10$. We first divide the regimes for the spin diffusion along the $\hat{\mathbf{x}}$ and $\hat{\mathbf{y}}$ directions, respectively. For the spin diffusion along the $\hat{\mathbf{x}}$ direction, the regimes for the system are divided into

$$\begin{aligned} &\text{IV}: l^c_{\tau,x} \lesssim l_\tau \lesssim l_\Omega, l_\alpha, \quad \text{when} \quad \Omega \lesssim 30E_r, \\ &\text{V}: l_\tau \lesssim l_\Omega, l_\alpha, l^c_{\tau,x}, \quad \text{when} \quad 30E_r \lesssim \Omega \lesssim 80E_r, \\ &\text{II}: l_\Omega \lesssim l_\tau \lesssim l_\alpha, \quad \text{when} \quad \Omega \gtrsim 80E_r, \end{aligned} \tag{37}$$

which are labeled by the red roman numbers with the boundaries indicated by the red crosses at the top frame of Fig. 4(a). For the spin diffusion along the $\hat{\mathbf{y}}$ direction, when $\Omega \lesssim 80E_r$ and $\Omega \gtrsim 80E_r$, the system lies in regimes IV and II, which are represented by the blue roman numbers with the boundaries indicated by the blue crosses at the bottom frame of Fig. 4(b). It is shown in Figs. 4(a) and 4(b) that in regime II, the transverse (longitudinal) diffusion length decreases slowly (increases) with the increase of the Zeeman field, represented by the red solid (blue dashed) curve with circles. This is because for the transverse spin diffusion along the $\hat{\mathbf{x}}$ direction ($\hat{\mathbf{y}}$ direction), in regime II, $L_T^x \approx 2l_\tau/\sqrt{3}$ ($L_T^y \approx \sqrt{2}l_\tau$), with the diffusion length marginally influenced by the Zeeman field. For the longitudinal spin diffusion, in regime II, $L_L^x \approx l_\tau l_\alpha/(\sqrt{3}l_\Omega)$ [$L_L^y \approx l_\tau l_\alpha/(\sqrt{3}l_\Omega)$], leading to the enhancement of the spin diffusion by the Zeeman field. We emphasize that this enhancement of the spin diffusion arises from the suppression of the longitudinal spin relaxation by the Zeeman field.

Finally, we emphasize the unique features in the Zeeman field dependence of the spin diffusions along the $\hat{\mathbf{x}}$ and $\hat{\mathbf{y}}$ directions, which can be observed in the experiment. These unique features arise in the longitudinal situation, i.e., the initial spin polarization is parallel to the Zeeman field, for the spin diffusion along both the $\hat{\mathbf{x}}$ and $\hat{\mathbf{y}}$ directions. On one hand, when the scattering is strong with the system in regime V, the longitudinal spin diffusion is marginally influenced by the Zeeman field; on the other hand, when the scattering is relatively weak and the Zeeman field is strong with the system in regime II, the spin-diffusion length is enhanced by the Zeeman field. These unique features can be understood in the framework of the *modified* drift-diffusion model addressed in Sec. III [49–54]. It is emphasized that here the drift-diffusion model is applicable, which is very different from the longitudinal spin diffusion along the $\hat{\mathbf{y}}$ direction in regimes III and IV [the red solid curve with circles in Fig. 3(d)], where the modified inhomogeneous broadening picture is used. We readdress that with the strong (weak) Zeeman and weak (strong) spin-orbit-coupled fields, the condition to apply the modified drift-diffusion model (modified inhomogeneous broadening picture) is that the initial spin polarization is parallel (perpendicular) to the larger field.

C. SOC strength dependence

In this part, we analyze the SOC strength dependence of the transverse and longitudinal spin diffusions along the $\hat{\mathbf{x}}$ [Fig. 5(a)] and $\hat{\mathbf{y}}$ directions [Fig. 5(b)]. It has been well understood from the drift-diffusion model that in the strong scattering regime, the spin-diffusion length is suppressed by the SOC ($l_s \propto 1/|\alpha|$) [49–54]. In our study, besides the suppression of the spin-diffusion length by the SOC, we find two unique features in the SOC strength dependence which cannot be derived from the oversimplified drift-diffusion

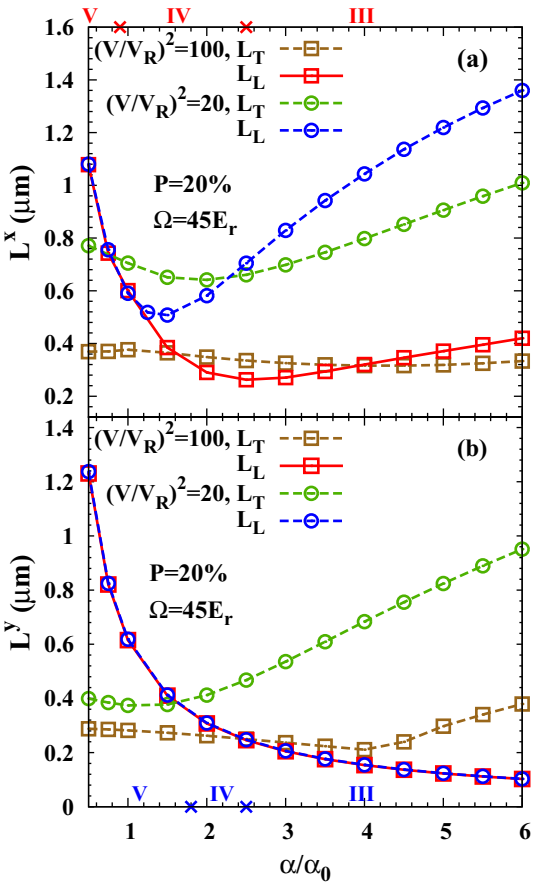

FIG. 5. (Color online) SOC dependence of the transverse and longitudinal spin diffusions along the (a) $\hat{\mathbf{x}}$ and (b) $\hat{\mathbf{y}}$ directions. The Zeeman field $\Omega = 45E_r$ and the spin polarization $P = 20\%$. The situations with the scattering strengths $(V/V_R)^2 = 100$ (squares) and $(V/V_R)^2 = 20$ (circles) calculated numerically are presented. The red (blue) roman numbers at the top (bottom) frame represent the different regimes for the spin diffusion along the $\hat{\mathbf{x}}$ direction ($\hat{\mathbf{y}}$ direction) when $(V/V_R)^2 = 20$ with the boundaries indicated by the red (blue) crosses.

model: The spin-diffusion length can be either marginally influenced or even enhanced by the SOC. These features can be realized when the system lies in the moderate and strong scattering regimes. Accordingly, in our calculation, the Zeeman field is set to be $\Omega = 45E_r$; the scattering strengths are set to be $(V/V_R)^2 = 100$ and $(V/V_R)^2 = 20$, respectively.

We first address the first unique feature, i.e., the marginal influence of the SOC on the spin diffusion. In Figs. 5(a) and 5(b), one observes that when $(V/V_R)^2 = 100$, whether the spin diffusion is along the $\hat{\mathbf{x}}$ or $\hat{\mathbf{y}}$ direction in the transverse configuration (the gray dashed curve with squares), when $\alpha \lesssim 4\alpha_0$, the spin diffusion length is marginally influenced by the SOC. This is because when $\alpha \lesssim 4\alpha_0$, the system lies in regime V with $L_T^x \approx \sqrt{2l_\tau l_\Omega/\sqrt{3}}$ ($L_L^x \approx \sqrt{\sqrt{3}l_\tau l_\Omega}$) for the transverse spin diffusion along the $\hat{\mathbf{x}}$ direction ($\hat{\mathbf{y}}$ direction). It is emphasized that this robustness of the spin diffusion to the SOC cannot be obtained from the drift-diffusion model [49–54]. As we have addressed in Sec. III, in the transverse spin diffusion in regime V, the inhomogeneous broadening has dominant influence on the spin diffusion.

We then analyze the second unique feature where the spin-diffusion length can be enhanced by the SOC. For the spin diffusion along the $\hat{\mathbf{x}}$ direction, it is shown in Fig. 5(a) by the green (blue) dashed curve with circles that when $(V/V_R)^2 = 20$ with $\alpha \gtrsim 2\alpha_0$, the transverse (longitudinal) spin diffusion is significantly enhanced by the SOC; for the spin diffusion along the $\hat{\mathbf{y}}$ direction, when $(V/V_R)^2 = 20$ with $\alpha \gtrsim 2\alpha_0$ the transverse spin-diffusion length also increases with the increase of the SOC (the green dashed curve with circles). This can be understood as follows. When $\alpha \gtrsim 2\alpha_0$, the system lies in regime III. Accordingly, for the transverse [longitudinal] spin diffusion along the $\hat{\mathbf{x}}$ direction, one obtains $L_T^x \approx l_\tau l_\Omega/(\sqrt{3}l_\alpha)$ [$L_L^x \approx \sqrt{2}l_\tau l_\Omega/(\sqrt{3}l_\alpha)$]; for the transverse spin diffusion along the $\hat{\mathbf{y}}$ direction, $L_T^x \approx \sqrt{3}l_\tau l_\Omega/(2l_\alpha)$. This unique feature is in contrast to the prediction of the drift-diffusion model [49–54].

In above sections, we have compared the analytical results [Eqs. (A9), (A10), (A15), (A19), and (A22)] with the numerical ones. Now, we address the general condition that the analytical results can be applied. It is noted that our analytical results are derived in the strong scattering regime with $l_\tau \lesssim l_\alpha, l_\Omega$ and then extended to the moderate scattering regime. The numerical calculations show that in the relatively strong and strong scattering regimes ($l_\tau \lesssim l_\alpha, l_\Omega$), the analytical results agree with the numerical ones fairly well; in the moderate scattering regime, the condition to use the analytical results is $l_\Omega \lesssim l_\tau < l_\alpha$ or $l_\alpha \lesssim l_\tau < l_\Omega$, which are close to the boundary between the moderate and relatively strong scattering regimes. However, even when the system is away from the boundary between the moderate and strong scattering regimes, the dependencies of the spin diffusion on the scattering strength, Zeeman field and SOC strength are qualitatively correct in the moderate scattering regimes.

V. CONCLUSION AND DISCUSSION

In conclusion, we have investigated the steady-state spin diffusion for the 3D ultracold spin-orbit-coupled ^{40}K gas by the KSBE approach [45], first analytically and then numerically. The spin diffusions along the $\hat{\mathbf{x}}$ and $\hat{\mathbf{y}}$ directions for the transverse ($\mathbf{P}||\hat{\mathbf{z}}$) and longitudinal ($\mathbf{P}||\hat{\mathbf{x}}$) configurations are studied. It is first shown analytically that the behaviors of the steady-state spin diffusion in the four configurations ($\hat{\mathbf{x}}$-T, $\hat{\mathbf{x}}$-L, $\hat{\mathbf{y}}$-T, and $\hat{\mathbf{y}}$-L) are determined by three characteristic lengths: the mean free path l_τ, the Zeeman oscillation length l_Ω, and the SOC oscillation length l_α. We have derived the spin-diffusion lengths for the spin diffusions in the four configurations in the strong scattering regime, which are then extended to the weak scattering one. We further find that in different limits, the complex analytical results can be reduced to different extremely simple forms, and, correspondingly, the system can be divided into different regimes. Specifically, it is revealed that by tuning the scattering strength, the system can be divided into *five* regimes: I, weak scattering regime ($l_\tau \gtrsim l_\Omega, l_\alpha$); II, Zeeman field-dominated moderate scattering regime ($l_\Omega \ll l_\tau \ll l_\alpha$); III, SOC-dominated moderate scat-

tering regime ($l_\alpha \ll l_\tau \ll l_\Omega$); IV, relatively strong scattering regime ($l_\tau^c \ll l_\tau \ll l_\Omega, l_\alpha$); V, strong scattering regime ($l_\tau \ll l_\Omega, l_\alpha, l_\tau^c$). In different regimes, the corresponding behaviors of the spacial evolution of the spin polarization in the steady state are very rich, showing different dependencies on the scattering strength, Zeeman field, and SOC strength. These dependencies are summarized in Table I (Table II) for the spin diffusion along the $\hat{\mathbf{x}}$ direction ($\hat{\mathbf{y}}$ direction). Then the scattering strength, Zeeman field, and SOC strength dependencies of the spin diffusions are numerically calculated and compared with the analytical ones. It is shown that the analytical results agree with the numerical ones fairly well in the relatively strong to strong scattering regime and the region close to the boundary between the moderate and relatively strong scattering regimes. However, it is found that even when the system is away from the strong scattering regime, the analytical results are still qualitatively correct in the moderate scattering regimes.

The rich behaviors of the spin diffusions in different regimes are hard to understand in the framework of the previous simple drift-diffusion model [49–54] or the direct inhomogeneous broadening [Eqs. (2) and (3)] picture [45–48,55] in the literature. In this work, we extend our previous inhomogeneous broadenings [Eqs. (2) and (3)] to the effective ones in Eqs. (20) and (21) [Eqs. (31) and (32)] for the spin diffusion along the $\hat{\mathbf{x}}$ direction [$\hat{\mathbf{y}}$ direction]. In the limit situation, we suggest reasonable pictures referred to as *modified* drift-diffusion model and *modified* inhomogeneous broadening picture to facilitate the understanding of the simple analytical results in Tables I and II. It is shown that the behaviors of the spin diffusions can be analyzed in the situation either with strong Zeeman and weak spin-orbit coupled fields (regimes II and V) or weak Zeeman and strong spin-orbit-coupled fields (regimes III and IV). When the spin polarization is parallel (perpendicular) to the larger field between the Zeeman and spin-orbit-coupled fields, the spin polarization cannot (can) rotate around the effective inhomogeneous broadening fields efficiently, and hence the *modified* drift-diffusion model (*modified* inhomogeneous broadening picture) can be used. In the modified drift-diffusion model, in the strong scattering regime, $\tau_s(\mathbf{k})$ remains the SRT in the conventional DP mechanism [29,30,32,45], whereas in the moderate scattering regime, $\tau_s(\mathbf{k})$ is replaced by the helix spin-flip rates determined in the helix space [31,40]. In the modified inhomogeneous broadening picture, the behavior of the spin diffusion is determined by the *effective* inhomogeneous broadenings together with the spin-conserving scattering. By means of the modified drift-diffusion model and modified inhomogeneous broadening picture, apart from regime IV, all the features in different regimes can be obtained. Below, we address several anomalous features of the spin diffusion, which are in contrast to *both* the simple drift-diffusion model and the direct inhomogeneous broadening picture.

In the scattering strength dependence, it is found that when $l_\alpha \ll l_\Omega$, the longitudinal spin diffusion along the $\hat{\mathbf{y}}$ direction is *robust* against the scattering even when the system is away from the strong scattering regime, which is in contrast to the simple drift-diffusion model. In that model, in the weak scattering regime, with $l_s \propto k\sqrt{\tau_k}/m$, the spin diffusion length is suppressed by the scattering. In the Zeeman field dependence, when the system is in regime II, the *longitudinal* spin diffusion is enhanced by the Zeeman field. This is in contrast to the prediction from the previous drift-diffusion model and the direct inhomogeneous broadening picture. In the simple drift-diffusion model, in the strong (weak) scattering regime, with $l_s \propto 1/(m|\alpha|)$ ($l_s \propto k\sqrt{\tau_k}/m$), it is obtained that the diffusion length is irrelevant to the Zeeman field. In the direct inhomogeneous broadening picture, the spin diffusion is suppressed due to the enhancement of the inhomogeneous broadening by the Zeeman field. Finally, in the SOC strength dependence, we find that the spin-diffusion length can also be enhanced by the SOC in regime III. This also goes beyond the prediction from the simple drift-diffusion model and the direct inhomogeneous broadening picture. In the simple drift-diffusion model, in the strong (weak) scattering regime, with $l_s \propto 1/(m|\alpha|)$ ($l_s \propto k\sqrt{\tau_k}/m$), the spin-diffusion length is suppressed (uninfluenced) by the SOC. In the direct inhomogeneous broadenings picture, the spin diffusion is uninfluenced (suppressed) for the spin diffusion along the $\hat{\mathbf{x}}$ direction ($\hat{\mathbf{y}}$ direction). All these anomalous behaviors have been well understood from our modified drift-diffusion model and/or modified inhomogeneous broadening picture.

We emphasize that for the longitudinal spin diffusion along the $\hat{\mathbf{y}}$ direction, the *robustness* against the scattering strength exists in a wide range including both the strong and the *weak* scattering regimes. It is noted that in the strong scattering regime, this feature has been predicted in the simple drift-diffusion model [49–53] and is also revealed in graphene by the KSBE approach [54]. In this work, we further extend it into the weak scattering regime. Moreover, it is found that in a wide range of the scattering, the corresponding diffusion length is only determined by the SOC strength, and hence is also irrelevant to the atom density and temperature. One expects similar behavior in symmetric (110) quantum wells under a weak in-plane magnetic field with similar SOC [39,40,66–70]. Moreover, the enhancement of the longitudinal spin diffusion by the Zeeman field has not yet been reported in the literature, which is also expected to be observed in symmetric (110) quantum wells when the Zeeman energy larger than the spin-orbit coupled one.

Finally, we further compare the pictures of the spin diffusion provided in this work to understand the calculated results and those in the literature. In the previous works, the spin diffusion in the *strong* scattering regime has been extensively studied in the system with SOC, including semiconductors [45,71–76], graphene [54,77–82], and recently monolayer MoS_2 [83]. The drift-diffusion model [49–53] and/or the inhomogeneous broadening picture [45–48,55] were used to understand the behaviors of the spin diffusion. In this work, the analytical results in the strong scattering regime are extended to the weak one and confirmed by the full numerical calculation. For the strong scattering regime, we further divide it into the relatively strong and strong scattering regimes, whereas for the weak scattering regime, we divide it into the moderate and weak scattering regimes. We find that all the anomalous behaviors revealed in this work appear in the moderate and relatively strong scattering regimes. Furthermore, our *modified* drift-diffusion model and/or *modified* inhomogeneous broadening picture are used to understand the behaviors of the spin

diffusion in all these regimes. It is found that in the moderate and strong scattering regimes, these pictures work well. However, in the relatively strong scattering regime, which lies in the crossover of the moderate and strong scattering regimes, these pictures fail to explain the behaviors of the spin diffusion along the $\hat{\mathbf{y}}$ direction. This is because for the drift-diffusion model, in the relatively strong scattering regime, it is too rough to consider the anisotropy between the diffusions along different directions [54]. Nevertheless, when the scattering is strong enough, this anisotropy in the spin-diffusion behavior vanishes. Whereas for the inhomogeneous broadening picture, in this regime there exists strong competition between the effective inhomogeneous broadening and scattering, which makes the behavior of the spin diffusion complicated [47,54,55].

ACKNOWLEDGMENTS

This work was supported by the National Natural Science Foundation of China under Grants No. 11334014 and No. 61411136001, the National Basic Research Program of China under Grant No. 2012CB922002, and the Strategic Priority Research Program of the Chinese Academy of Sciences under Grant No. XDB01000000.

APPENDIX: ANALYTICAL ANALYSIS

We analytically derive the transverse and longitudinal spin-diffusion lengths for the spin diffusions along the $\hat{\mathbf{x}}$ and $\hat{\mathbf{y}}$ directions based on the KSBEs [Eq. (12)].

Generally, the density matrix depends on both the zenith (between $\mathbf{k}$ and $\hat{x}$ axis) and azimuth (between $\mathbf{k}$ and $\hat{y}$ axis in the $\hat{y}$-$\hat{z}$ plane) angles $\theta_{\mathbf{k}}$ and $\phi_{\mathbf{k}}$ in 3D. However, with the specific form of the SOC [Eq. (1)] and isotropic scattering terms [Eq. (9)], we can define the quantity

$$\bar{\rho}_{\mathbf{k}} = \frac{1}{2\pi}\int_0^{2\pi} d\phi_{\mathbf{k}}\rho_{\mathbf{k}}, \tag{A1}$$

which is averaged over the azimuth angle $\phi_{\mathbf{k}}$, to describe the kinetics of the density matrix [31]. Accordingly, the KSBEs in the steady state become

$$\frac{k_\xi}{m}\frac{\partial\bar{\rho}_{\mathbf{k}}(\mathbf{r})}{\partial\xi} + i[\Omega\sigma_x/2,\bar{\rho}_{\mathbf{k}}(\mathbf{r})] + i[\alpha k_x\sigma_z/2,\bar{\rho}_{\mathbf{k}}(\mathbf{r})] + \sum_{\mathbf{k}'} W_{\mathbf{k}\mathbf{k}'}[\bar{\rho}_{\mathbf{k}}(\mathbf{r}) - \bar{\rho}_{\mathbf{k}'}(\mathbf{r})] = 0, \tag{A2}$$

in which $\bar{\rho}_{\mathbf{k}}(\mathbf{r})$ only depends on $\theta_{\mathbf{k}}$.

1. Spin diffusion along the $\hat{\mathbf{x}}$ direction

For the spin diffusion along the $\hat{\mathbf{x}}$ direction, $\bar{\rho}_{\mathbf{k}}$ is expanded by the Legendre function, which is written as

$$\bar{\rho}_{\mathbf{k}} = \sum_l \bar{\rho}_k^l C_l^0 P_l(\cos\theta_{\mathbf{k}}), \tag{A3}$$

with $C_l^0 = \sqrt{(2l+1)/(4\pi)}$. Accordingly, the dynamical equation for $\bar{\rho}_k^l$ is written as Eq. (13). With the spin vector defined by $\bar{\mathbf{S}}_k^l = \mathrm{Tr}[\bar{\rho}_k^l\boldsymbol{\sigma}]$, the equations for the spin vectors can be obtained. By further keeping the zeroth and first orders ($l = 0,1$), the equation for the vector $\bar{\mathbf{S}}_k = (\bar{\mathbf{S}}_{k,x}^0,\bar{\mathbf{S}}_{k,y}^0,\bar{\mathbf{S}}_{k,z}^0,\bar{\mathbf{S}}_{k,x}^1,\bar{\mathbf{S}}_{k,y}^1,\bar{\mathbf{S}}_{k,z}^1)^T$ is written as

$$\partial_x\bar{\mathbf{S}}_k + U_x\bar{\mathbf{S}}_k = 0, \tag{A4}$$

with

$$U_x = \begin{pmatrix} 0 & 1/l_\alpha & 0 & \sqrt{3}/l_\tau & 0 & 0 \\ -1/l_\alpha & 0 & 0 & 0 & \sqrt{3}/l_\tau & 1/l_\Omega \\ 0 & 0 & 0 & 0 & -1/l_\Omega & \sqrt{3}/l_\tau \\ 0 & 0 & 0 & 0 & 1/l_\alpha & 0 \\ 0 & 0 & 1/l_\Omega & -1/l_\alpha & 0 & 0 \\ 0 & -1/l_\Omega & 0 & 0 & 0 & 0 \end{pmatrix}. \tag{A5}$$

From Eq. (A5), the spin-diffusion and oscillation lengths can be found from the eigenvalues of U_x denoted by λ_x, which satisfy

$$\lambda_x^6 + a\lambda_x^4 + b\lambda_x^2 + c = 0, \tag{A6}$$

with $a = 2/l_\Omega^2 + 2/l_\alpha^2$, $b = 3/(l_\tau l_\Omega)^2 + 1/l_\Omega^4 + 2/(l_\Omega l_\alpha)^2 + 1/l_\alpha^4$, and $c = -3/(l_\tau l_\Omega l_\alpha)^2$. In Eq. (A6), the real and imaginary parts of $1/\lambda_x$ correspond to the diffusion length and oscillation length, respectively.

With $\Delta = (q/2)^2 + (p/3)^3$, where $q = 2a^3/27 - ab/3 + c$ and $p = b - a^2/3$, it is demonstrated that in the moderate and strong scattering regimes, Δ is always larger than zero. Therefore, there are one real root (Λ_{re}) and two complex conjugate roots ($\Lambda_{\mathrm{im},\pm}$) for λ_x^2 in Eq. (A6), which are written as

$$\Lambda_{\mathrm{re}} = \sqrt[3]{-q/2-\sqrt{\Delta}} + \sqrt[3]{-q/2+\sqrt{\Delta}}, \tag{A7}$$

$$\Lambda_{\mathrm{im},\pm} = -(1/2)(\sqrt[3]{-q/2-\sqrt{\Delta}} + \sqrt[3]{-q/2+\sqrt{\Delta}}) \pm (\sqrt{3}i/2)(\sqrt[3]{-q/2-\sqrt{\Delta}} - \sqrt[3]{-q/2+\sqrt{\Delta}}). \tag{A8}$$

Accordingly, the spin-diffusion length for the single exponential decay, the spin-diffusion length for the oscillation decay and the spin oscillation length are given by

$$L_s^x = 1/\sqrt{\Lambda_{\mathrm{re}}}, \tag{A9}$$

$$L_o^x = \sqrt{2}/\sqrt{\Lambda_{\mathrm{re}} + \sqrt{\Lambda_{\mathrm{re}}^2 + |\Lambda_{\mathrm{im},+} - \Lambda_{\mathrm{im},-}|^2/3}}, \tag{A10}$$

$$l_o^x = 2\sqrt{3}L_o^x/|\Lambda_{\mathrm{im},+} - \Lambda_{\mathrm{im},-}|. \tag{A11}$$

2. Spin diffusion along the $\hat{\mathbf{y}}$ direction

For the spin diffusion along the $\hat{\mathbf{y}}$ direction, $\bar{\rho}_{\mathbf{k}}$ is expanded by the Fourier function, which is denoted by

$$\bar{\rho}_{\mathbf{k}} = \sum_l \tilde{\rho}_k^l \exp(il\theta_{\mathbf{k}}). \tag{A12}$$

The corresponding dynamical equation for $\tilde{\rho}_k^l$ is written as Eq. (22). By keeping the zeroth and first orders ($l = 0,1$), the equation for the vector $\tilde{\mathbf{S}}_k = (\tilde{\mathbf{S}}^0_{k,x}, \tilde{\mathbf{S}}^1_{k,x} - \tilde{\mathbf{S}}^{-1}_{k,x}, \tilde{\mathbf{S}}^0_{k,y}, \tilde{\mathbf{S}}^0_{k,z}, \tilde{\mathbf{S}}^1_{k,y} - \tilde{\mathbf{S}}^{-1}_{k,y}, \tilde{\mathbf{S}}^1_{k,z} - \tilde{\mathbf{S}}^{-1}_{k,z})^T$ is written as

$$\partial_y \tilde{\mathbf{S}}_k + U_y \tilde{\mathbf{S}}_k = 0, \tag{A13}$$

where

$$U_y = \begin{pmatrix} 0 & \frac{i}{l_\tau} & 0 & 0 & 0 & 0 \\ \frac{-i}{l_\tau^2/(3l_\Omega^2)+1}\frac{l_\tau}{l_\alpha^2} & 0 & 0 & 0 & 0 & 0 \\ 0 & 0 & 0 & 0 & \frac{i}{l_\tau} & \frac{i}{\sqrt{3}l_\Omega} \\ 0 & 0 & 0 & 0 & -\frac{i}{\sqrt{3}l_\Omega} & \frac{i}{l_\tau} \\ 0 & 0 & -\frac{il_\tau}{l_\alpha^2} & -\frac{2i}{\sqrt{3}l_\Omega} & 0 & 0 \\ 0 & 0 & \frac{2i}{\sqrt{3}l_\Omega} & 0 & 0 & 0 \end{pmatrix}. \tag{A14}$$

In above equation, it is noted that the top-left 2×2 and bottom-right 4×4 blocks $U_y^{\text{u-l}}$ and $U_y^{\text{d-r}}$, which describe the spin diffusion for $\mathbf{S}_x$ and $\mathbf{S}_y/\mathbf{S}_z$, are decoupled from each other.

Accordingly, from the eigenvalues of $U_y^{\text{u-l}}$, the spin-diffusion length for $\mathbf{S}_x$ is found to be

$$L_L^y = l_\alpha \sqrt{l_\tau^2/(3l_\Omega^2) + 1}. \tag{A15}$$

From $U_y^{\text{d-r}}$, it is found that the four eigenvalues λ_y satisfy

$$\lambda_y^4 + \left[4/(3l_\Omega^2) - 1/l_\alpha^2\right]\lambda_y^2 + 4/(3l_\Omega^2 l_\tau^2) + 4/(9l_\Omega^4) = 0. \tag{A16}$$

From Eq. (A16), when $1/l_\alpha^4 - 8/(3l_\Omega^2)(1/l_\alpha^2 + 2/l_\tau^2) \geqslant 0$, there are four real roots, among which the two positive ones read

$$|\lambda_y^{\pm}| = \sqrt{\frac{1}{2l_\alpha^2} - \frac{2}{3l_\Omega^2} \pm \sqrt{\frac{1}{4l_\alpha^4} - \frac{2}{3l_\Omega^2 l_\alpha^2} - \frac{4}{3l_\Omega^2 l_\tau^2}}}. \tag{A17}$$

Accordingly, the steady-state spin polarization $\mathbf{S}_y$ or $\mathbf{S}_z$ is limited by the biexponential decay, with the diffusion length being

$$L_T^{y,+} = 1/|\lambda_y^+|, \tag{A18}$$

$$L_T^{y,-} = 1/|\lambda_y^-|, \tag{A19}$$

respectively. Otherwise, when $1/l_\alpha^4 - 8/(3l_\Omega^2)(1/l_\alpha^2 + 2/l_\tau^2) < 0$, the four roots for λ_y are complex. Specifically, the real part of the roots for Eq. (A16) is identical, which is written as

$$\lambda_y^{\text{re}} = \sqrt{1/(4l_\alpha^2) - 1/(3l_\Omega^2) + \sqrt{1/(9l_\Omega^4) + 1/(3l_\Omega^2 l_\tau^2)}}. \tag{A20}$$

The complex part of the roots (absolute value) for Eq. (A16) is

$$|\lambda_y^{\text{im}}| = \sqrt{2/(3l_\Omega^2)(1/l_\alpha^2 + 2/l_\tau^2) - 1/(4l_\alpha^4)}. \tag{A21}$$

Therefore, the steady-state spin polarization $\mathbf{S}_y$ or $\mathbf{S}_z$ is determined by the oscillation decay with the decay length and oscillation length being

$$L_T^y = 1/\lambda_y^{\text{re}}, \tag{A22}$$

$$l_T^y = 2\lambda_y^{\text{re}}/|\lambda_y^{\text{im}}|, \tag{A23}$$

respectively.

[1] J. Y. Vaishnav and C. W. Clark, Phys. Rev. Lett. **100**, 153002 (2008).

[2] J. Y. Zhang, S. C. Ji, Z. Chen, L. Zhang, Z. D. Du, B. Yan, G. S. Pan, B. Zhao, Y. J. Deng, H. Zhai, S. Chen, and J. W. Pan, Phys. Rev. Lett. **109**, 115301 (2012).

[3] C. Qu, C. Hamner, M. Gong, C. Zhang, and P. Engels, Phys. Rev. A **88**, 021604(R) (2013).

[4] L. J. LeBlanc, M. C. Beeler, K. J. García, A. R. Perry, S. Sugawa, R. A. Williams, and I. B. Spielman, New J. Phys. **15**, 073011 (2013).

[5] M. C. Beeler, R. A. Williams, K. J. García, L. J. LeBlanc, A. R. Perry, and I. B. Spielman, Nature (London) **498**, 201 (2013).

[6] P. L. Pedersen, M. Gajdacz, F. Deuretzbacher, L. Santos, C. Klempt, J. F. Sherson, A. J. Hilliard, and J. J. Arlt, Phys. Rev. A **89**, 051603(R) (2014).

[7] Y. J. Lin, K. J. García, and I. B. Spielman, Nature (London) **471**, 83 (2011).

[8] K. Jiménez-García, L. J. LeBlanc, R. A. Williams, M. C. Beeler, C. Qu, M. Gong, C. Zhang, and I. B. Spielman, Phys. Rev. Lett. **114**, 125301 (2015).

[9] A. Sommer, M. Ku, and M. W. Zwierlein, New J. Phys. **13**, 055009 (2011).

[10] H. Heiselberg, Phys. Rev. Lett. **108**, 245303 (2012).

[11] O. Goulko, F. Chevy, and C. Lobo, Phys. Rev. Lett. **111**, 190402 (2013).

[12] C. Cao, E. Elliott, J. Joseph, H. Wu, J. Petricka, T. Schäfer, and J. E. Thomas, Science **331**, 58 (2011).

[13] A. Sommer, M. Ku, G. Roati, and M. W. Zwierlein, Nature (London) **472**, 201 (2011).

[14] G. M. Bruun, New J. Phys. **13**, 035005 (2011).

[15] T. Enss and R. Haussmann, Phys. Rev. Lett. **109**, 195303 (2012).

[16] T. Enss, Phys. Rev. A **88**, 033630 (2013).
[17] A. J. Leggett and M. J. Rice, Phys. Rev. Lett. **20**, 586 (1968); A. J. Leggett, J. Phys. C **3**, 448 (1970).
[18] M. Koschorreck, D. Pertot, E. Vogt, and M. Köhl, Nat. Phys. **9**, 405 (2013).
[19] A. B. Bardon, S. Beattie, C. Luciuk, W. Cairncross, D. Fine, N. S. Cheng, G. J. A. Edge, E. Taylor, S. Zhang, S. Trotzky, and J. H. Thywissen, Science **344**, 722 (2014).
[20] S. Trotzky, S. Beattie, C. Luciuk, S. Smale, A. B. Bardon, T. Enss, E. Taylor, S. Zhang, and J. H. Thywissen, Phys. Rev. Lett. **114**, 015301 (2015).
[21] T. Enss, Phys. Rev. A **91**, 023614 (2015).
[22] X. Du, L. Luo, B. Clancy, and J. E. Thomas, Phys. Rev. Lett. **101**, 150401 (2008).
[23] F. Piéchon, J. N. Fuchs, and F. Laloë, Phys. Rev. Lett. **102**, 215301 (2009).
[24] S. S. Natu and E. J. Mueller, Phys. Rev. A **79**, 051601(R) (2009).
[25] X. Du, Y. Zhang, J. Petricka, and J. E. Thomas, Phys. Rev. Lett. **103**, 010401 (2009).
[26] P. Wang, Z. Q. Yu, Z. Fu, J. Miao, L. Huang, S. Chai, H. Zhai, and J. Zhang, Phys. Rev. Lett. **109**, 095301 (2012).
[27] L. W. Cheuk, A. T. Sommer, Z. Hadzibabic, T. Yefsah, W. S. Bakr, and M. W. Zwierlein, Phys. Rev. Lett. **109**, 095302 (2012).
[28] U. Ebling, J. S. Krauser, N. Fläschner, K. Sengstock, C. Becker, M. Lewenstein, and A. Eckardt, Phys. Rev. X **4**, 021011 (2014).
[29] I. V. Tokatly and E. Ya. Sherman, Phys. Rev. A **87**, 041602(R) (2013).
[30] S. S. Natu and S. Das Sarma, Phys. Rev. A **88**, 033613 (2013).
[31] T. Yu and M. W. Wu, Phys. Rev. A **88**, 043634 (2013).
[32] J. Radić, S. S. Natu, and V. Galitski, Phys. Rev. Lett. **112**, 095302 (2014).
[33] I. Bloch, J. Dalibard, and W. Zwerger, Rev. Mod. Phys. **80**, 885 (2008).
[34] S. S. Kondov, W. R. McGehee, J. J. Zirbel, and B. DeMarco, Science **334**, 66 (2011).
[35] F. Jendrzejewski, A. Bernard, K. Müller, P. Cheinet, V. Josse, M. Piraud, L. Pezzé, L. S. Palencia, A. Aspect, and P. Bouyer, Nat. Phys. **8**, 398 (2012).
[36] G. Semeghini, M. Landini, P. Castilho, S. Roy, G. Spagnolli, A. Trenkwalder, M. Fattori, M. Inguscio, and G. Modugno, arXiv:1404.3528.
[37] D. Clément, A. F. Varón, J. A. Retter, L. S. Palencia, A. Aspect, and P. Bouyer, New J. Phys. **8**, 165 (2006).
[38] M. Piraud, L. Pezzé, and L. S. Palencia, New J. Phys. **15**, 075007 (2013).
[39] Y. Zhou, T. Yu, and M. W. Wu, Phys. Rev. B **87**, 245304 (2013).
[40] T. Yu and M. W. Wu, Phys. Rev. B **89**, 045303 (2014).
[41] M. I. D'yakonov and V. I. Perel', Zh. Eksp. Teor. Fiz. **60**, 1954 (1971) [Sov. Phys. JETP **33**, 1053 (1971)].
[42] Y. Yafet, Phys. Rev. **85**, 478 (1952).
[43] R. J. Elliott, Phys. Rev. **96**, 266 (1954).
[44] J.-P. Brantut, J. Meineke, D. Stadler, S. Krinner, and T. Esslinger, Science **337**, 1069 (2012).
[45] M. W. Wu, J. H. Jiang, and M. Q. Weng, Phys. Rep. **493**, 61 (2010).
[46] M. W. Wu and C. Z. Ning, Eur. Phys. J. B. **18**, 373 (2000); M. W. Wu, J. Phys. Soc. Jpn. **70**, 2195 (2001).
[47] J. L. Cheng and M. W. Wu, J. Appl. Phys. **101**, 073702 (2007).
[48] M. Q. Weng and M. W. Wu, Phys. Rev. B **66**, 235109 (2002); J. Appl. Phys. **93**, 410 (2003).
[49] M. Ziese and M. J. Thornton (eds.), *Spin Electronics* (Springer, Berlin, 2001).
[50] Z. G. Yu and M. E. Flatté, Phys. Rev. B **66**, 201202(R) (2002).
[51] I. Zutić, J. Fabian, and S. Das Sarma, Phys. Rev. Lett. **88**, 066603 (2002).
[52] J. Fabian, I. Zutić, and S. Das Sarma, Phys. Rev. B **66**, 165301 (2002).
[53] J. Fabian, A. M. Abiague, C. Ertler, P. Stano, and I. Zutić, Acta Phys. Slov. **57**, 565 (2007).
[54] P. Zhang and M. W. Wu, Phys. Rev. B **84**, 045304 (2011).
[55] J. L. Cheng, M. W. Wu, and I. C. da Cunha Lima, Phys. Rev. B **75**, 205328 (2007).
[56] C. A. Regal, C. Ticknor, J. L. Bohn, and D. S. Jin, Phys. Rev. Lett. **90**, 053201 (2003).
[57] M. Egorov, B. Opanchuk, P. Drummond, B. V. Hall, P. Hannaford, and A. I. Sidorov, Phys. Rev. A **87**, 053614 (2013).
[58] T. Ozawa, L. P. Pitaevskii, and S. Stringari, Phys. Rev. A **87**, 063610 (2013).
[59] R. A. Williams, M. C. Beeler, L. J. LeBlanc, K. Jimenez-García, and I. B. Spielman, Phys. Rev. Lett. **111**, 095301 (2013).
[60] M. W. Wu and H. Metiu, Phys. Rev. B **61**, 2945 (2000).
[61] H. Haug and A. P. Jauho, *Quantum Kinetics in Transport and Optics of Semiconductors* (Springer, Berlin, 1996).
[62] M. Q. Weng and M. W. Wu, Phys. Rev. B **68**, 075312 (2003).
[63] J. H. Jiang and M. W. Wu, Phys. Rev. B **79**, 125206 (2009).
[64] A. F. Ioffe and A. R. Regel, Prog. Semicond. **4**, 237 (1960).
[65] P. W. Anderson, Phys. Rev. **109**, 1492 (1958).
[66] Y. Ohno, R. Terauchi, T. Adachi, F. Matsukura, and H. Ohno, Phys. Rev. Lett. **83**, 4196 (1999); Phys. E (Amsterdam, Neth.) **6**, 817 (2000); T. Adachi, Y. Ohno, F. Matsukura, and H. Ohno, *ibid.* **10**, 36 (2001).
[67] M. W. Wu and M. Kuwata-Gonokami, Solid State Commun. **121**, 509 (2002).
[68] S. Döhrmann, D. Hägele, J. Rudolph, M. Bichler, D. Schuh, and M. Oestreich, Phys. Rev. Lett. **93**, 147405 (2004).
[69] G. M. Müller, M. Römer, D. Schuh, W. Wegscheider, J. Hübner, and M. Oestreich, Phys. Rev. Lett. **101**, 206601 (2008).
[70] I. V. Tokatly and E. Y. Sherman, Phys. Rev. B **82**, 161305(R) (2010).
[71] T. Ando, A. B. Fowler, and F. Stern, Rev. Mod. Phys. **54**, 437 (1982).
[72] F. Meier and B. P. Zakharchenya, *Optical Orientation* (North-Holland, Amsterdam, 1984).
[73] D. D. Awschalom, D. Loss, and N. Samarth (eds.), *Semiconductor Spintronics and Quantum Computation* (Springer, Berlin, 2002).
[74] I. Žutić, J. Fabian, and S. D. Sarma, Rev. Mod. Phys. **76**, 323 (2004).
[75] Edited by M. I. D'yakonov, *Spin Physics in Semiconductors* (Springer, Berlin, 2008).
[76] T. Korn, Phys. Rep. **494**, 415 (2010).
[77] N. Tombros, C. Jozsa, M. Popinciuc, H. T. Jonkman, and B. J. van Wees, Nature (London) **448**, 571 (2007).

[78] C. Ertler, S. Konschuh, M. Gmitra, and J. Fabian, Phys. Rev. B **80**, 041405(R) (2009).

[79] K. Pi, W. Han, K. M. McCreary, A. G. Swartz, Y. Li, and R. K. Kawakami, Phys. Rev. Lett. **104**, 187201 (2010).

[80] M. H. D. Guimarães, A. Veligura, P. J. Zomer, T. Maassen, I. J. Vera-Marun, N. Tombros, and B. J. van Wees, Nano Lett. **2012**, 3512 (2012).

[81] W. Han, K. M. McCreary, K. Pi, W. H. Wang, Y. Li, H. Wen, J. R. Chen, and R. K. Kawakami, J. Magn. Magn. Mater. **324**, 369 (2012).

[82] A. Dankert, M. V. Kamalakar, J. Bergsten, and S. P. Dash, Appl. Phys. Lett. **104**, 192403 (2014).

[83] L. Wang and M. W. Wu, Phys. Rev. B **89**, 205401 (2014).